Mixed-Flow Turbofan Engine Model for the Conceptual Design of Sustainable Supersonic Airplanes

aerospace

MDPI

Article

Mixed-Flow Turbofan Engine Model for the Conceptual Design of Sustainable Supersonic Airplanes

Grazia Piccirillo [1], Antonio Gregorio [1], Roberta Fusaro [2], Davide Ferretto [1,*] and Nicole Viola [2]

[1] Department of Mechanical and Aerospace Engineering, Politecnico di Torino, Corso Duca Degli Abruzzi 24, 10129 Torino, Italy; grazia.piccirillo@polito.it (G.P.); antonio.gregorio@polito.it (A.G.)
[2] Department of Management and Production Engineering, Politecnico di Torino, Corso Duca Degli Abruzzi 24, 10129 Torino, Italy; roberta.fusaro@polito.it (R.F.); nicole.viola@polito.it (N.V.)
* Correspondence: davide.ferretto@polito.it

Abstract: Current research efforts on commercial supersonic flight aim to overcome past challenges by designing a new generation of sustainable supersonic airplanes. Achieving this goal requires careful consideration of the propulsion system during the design process. This study proposes a mixed-flow turbofan engine model coupled with emission estimation routines to increase the reliability of the conceptual design of future supersonic aircraft. The model enables parametric analyses by analyzing variations in main engine design parameters (π_c, π_f, BPR) as function of the system and mission requirements, such as the Mach number, and suggesting applicability boundaries. The overall methodology was applied to a low-boom Mach 1.5 case study, allowing for both on-design and off-design analyses and generating a propulsive database to support preliminary mission simulations and chemical emission estimation. Finally, the accuracy and reliability of the engine model was validated against GSP 11 data for a generic mixed-flow turbofan engine. A modified version of the Fuel Flow Method, originally developed by Boeing, allows for emissions estimation throughout the mission for a supersonic engine using biofuels. The application of the methodology led to the definition of an engine with a π_c of 30 and BPR of 0.7 for the selected case study, which was successful in meeting the initial mission requirements.

Keywords: mixed-flow turbofan engine; supersonic aircraft; conceptual design

Citation: Piccirillo, G.; Gregorio, A.; Fusaro, R.; Ferretto, D.; Viola, N. Mixed-Flow Turbofan Engine Model for the Conceptual Design of Sustainable Supersonic Airplanes. *Aerospace* **2024**, *11*, 740. https://doi.org/10.3390/aerospace11090740

Academic Editor: Dimitri Mavris

Received: 7 August 2024
Revised: 31 August 2024
Accepted: 3 September 2024
Published: 10 September 2024

1. Introduction

Although the Concorde, the only commercial supersonic aircraft to achieve technological success, was retired due to environmental and economic concerns, research into supersonic flight has continued. Today, efforts are dedicated to tackling the unresolved challenges of the past, leveraging previous experiences to guide the design of next-generation supersonic airplanes [1,2].

A common thread of recent research initiatives [3–7] is the consideration of environmental sustainability as an essential requirement in supersonic aircraft design [8]. Future concepts must adhere to current subsonic environmental standards, including stringent noise and emissions regulations compared to those applicable to the Concorde, while also minimizing sonic booms to enable overland flights, thereby enhancing economic viability and public acceptance [9–11]. Achieving these goals requires careful consideration of the propulsion system during design process, as it significantly affects the environmental performance and economic viability of the aircraft [12,13].

The design of an engine for future commercial supersonic aircraft presents several technical challenges, and the need to find the optimal solution has driven the exploration of various viable solutions since the beginning of research into the next generation of these vehicles. Specifically, advanced supersonic propulsion technologies have been investigated by NASA during the High-Speed Research (HSR) program in the 1980s [14], marking

an initial comprehensive research effort in the field. Over the years, subsequent studies have focused on different aspects of propulsion system design for supersonic transport, achieving a deeper understanding of the features that this system should have. Supersonic propulsion systems shall satisfy demanding requirements, such as a high thrust-to-weight ratio and ensure high propulsive efficiency across both subsonic and supersonic flight regimes [15]. This objective also entails the proper design of intake and exhaust systems to prevent inlet unstart and minimize pressure losses under all flight conditions [16,17]. Typically, achieving high turbine inlet temperatures is crucial to generating the required levels of thrust. Therefore, advanced materials capable of withstanding high temperatures and vibrations over extended periods while remaining cost-effective for turbomachinery components are required to ensure the feasibility of these concepts [18]. Addressing noise reduction during take-off and landing, as well as minimizing chemical emissions from engine exhaust, particularly nitrogen oxide, which can contribute to ozone depletion, are environmental concerns and are inherently tied to technical advancements [19,20]. The effective integration of the propulsion system plays a critical role in minimizing drag and mitigating sonic boom. Indeed, engine integration influences the near-field pressure signature and resulting ground-level sonic boom intensity of a supersonic aircraft [21].

Given the complexity of designing propulsion systems for supersonic aircraft and the significant impact this has on the overall design, this discipline is typically incorporated into multidisciplinary and integrated frameworks for supersonic aircraft design [11,22,23]. Generally, these frameworks couple different software tools related to specific design areas to provide a holistic perspective during the design process, including environmental and/or economic implications.

For propulsion system design, the most widely used tool is NPSS (Numerical Propulsion System Simulation) [24]. Developed jointly by NASA and the U.S. aerospace industry, NPSS is the accepted state-of-the-art software for airbreathing engine cycle performance analysis and has been integrated with other software tools to enable the analysis of supersonic aircraft case studies [11,25]. Additionally, there is PROOSIS, an object-oriented simulation environment for modeling gas turbine engines [26], and GasTurb [27], a user-friendly gas turbine performance simulation code that can evaluate the thermodynamic cycle of a predefined set of engine architectures at both design and off-design stages. Numerous other tools have been developed in academia and industry for propulsion system modeling, such as the GSP (Gas turbine Simulation Program) [28] by the Netherlands Research Laboratory (NLR).

However, the software tools and models implemented are not widely available commercially or, in most cases, were not originally conceived to tackle the design of commercial supersonic aircraft. Additionally, engine modeling tools typically need to interface with other software to provide a comprehensive assessment that involves, for instance, chemical and noise emissions, among other factors. As a result, there is a lack of propulsion system models capable of specifically and rapidly addressing the aspects of civil supersonic aircraft during the conceptual design stage. This gap hinders the application of a seamless and comprehensive multidisciplinary approach from the earliest stages of aircraft design.

Therefore, this paper proposes a rapid, replicable, and flexible engine model for the conceptual design of future, and more sustainable, supersonic aircraft. The engine model is based on the most promising thermodynamic cycle identified in the literature for these applications, i.e., mixed-flow turbofan engines. It is specifically tailored for commercial supersonic aircraft and was designed to be adaptable, handling different supersonic aircraft requirements with cruise Mach numbers ranging from 1.5 to 3. This means that this model can enable multiple analyses, essential for trade studies during the early design stages. Additionally, to facilitate environmental assessment analysis and support eco-friendly design goals, the model integrates emissions estimation analyses. To enable emissions estimation at an acceptable level of accuracy during conceptual design, a modified version of the Fuel Flow Method, originally developed by Boeing, is used [29,30]. This allows for emissions estimation throughout the mission for a supersonic engine

using biofuels. The developed algorithms were designed for seamless integration into the Rapid Aircraft Prototyping tool, ASTRID-H 2.0 (Aircraft on-board Systems sizing and TRade-off analysis in Initial Design), a proprietary tool developed by the research group which the authors belong to at the Polytechnic University of Turin. ASTRID-H 2.0 will subsequently be integrated into the ESATTO (Environmentally Sustainable AircrafT Trajectory and Operations) modeling framework, a multidisciplinary platform developed in the MORE&LESS (MDO and REgulations for Low-boom and Environmentally Sustainable Supersonic aviation) project [6] for comprehensive environmental assessments of future supersonic aircraft.

Sections 2 and 3 provide an overview of the overall conceptual design methodology and its implementation in the ASTRID-H 2.0 tool. Section 4 offers a detailed description of the adopted propulsion system model, including the emission modeling approach, integrated to provide preliminary emission estimations in terms of emission indices. Afterwards, the results of the parametric analysis, which varied the cruise Mach number from 1.5 to 3, are presented to evaluate the technical limitations of using the proposed engine cycle within this range of flight speeds. The complete design methodology was then applied to a low-boom case study cruising at Mach 1.5. This case-study was chosen for its potential to more easily align with current environmental standards and offer viable high-speed travel solutions [31,32]. Therefore, on-design and off-design analyses were performed, analyzing the results of the propulsive database generated from the off-design simulations. The accuracy and reliability of the engine model was validated against GSP 11 data for a generic mixed-flow turbofan engine. The propulsive database was finally used to conduct mission simulations and subsequent emissions estimations. This process provided preliminary insights into the performance and environmental assessments of this concept, and also evaluated the limitations of the methodology for future improvements.

2. Overall Design Methodology

The most effective way to address the challenging design of an efficient, environmentally friendly, and economically viable supersonic transport aircraft is through an integrated and multidisciplinary approach, which allows for a detailed examination of the interactions between various design areas. Frameworks implementing this approach might be focused on key design areas, such as aerodynamics, structures, and performance, to assess the impact of their requirements on specific factors like mission range [33] and sonic boom minimization [34], and may also be complemented with cost or environmental assessments [11,23]. Drawing inspiration from these methods, this study aimed to apply a multidisciplinary design methodology to evaluate aircraft emissions for future sustainable supersonic concepts. This includes the development and integration of an engine model tailored for supersonic propulsion systems that can directly enable environmental analyses. The multidisciplinary approach applied in this study is illustrated in Figure 1.

The workflow begins with the definition of the high-level requirements, which include performance criteria (payload, cruise Mach number, range, type of fuel, and/or SFC) and environmental factors, specifically chemical emissions evaluated through emission indices. Based on these requirements, the preliminary aircraft design is developed, including the definition of geometry and weights, and a reference mission profile. The performance requirements are preliminary verified using the matching chart tool. This tool embeds a low-fidelity estimation of the aerodynamics coefficients and fuel consumption for each phase of the reference profile, with the objective of obtaining, through an iterative loop, the thrust-to-weight ratio (T/W) and the wing loading (W/S_w) that meet the mission requirements. Once this phase is complete, the initial aircraft design is consolidated, allowing for a more accurate characterization of the aerodynamic and propulsive performances. To achieve this, a more detailed aircraft geometry is required, such as a CAD model. This allows for an aerodynamic characterization of the aircraft moving towards higher-fidelity models, such as CFD analysis, to determine the aerodynamic coefficients at different Mach numbers and angles of attack, generating an aerodynamic database for mission analysis [35].

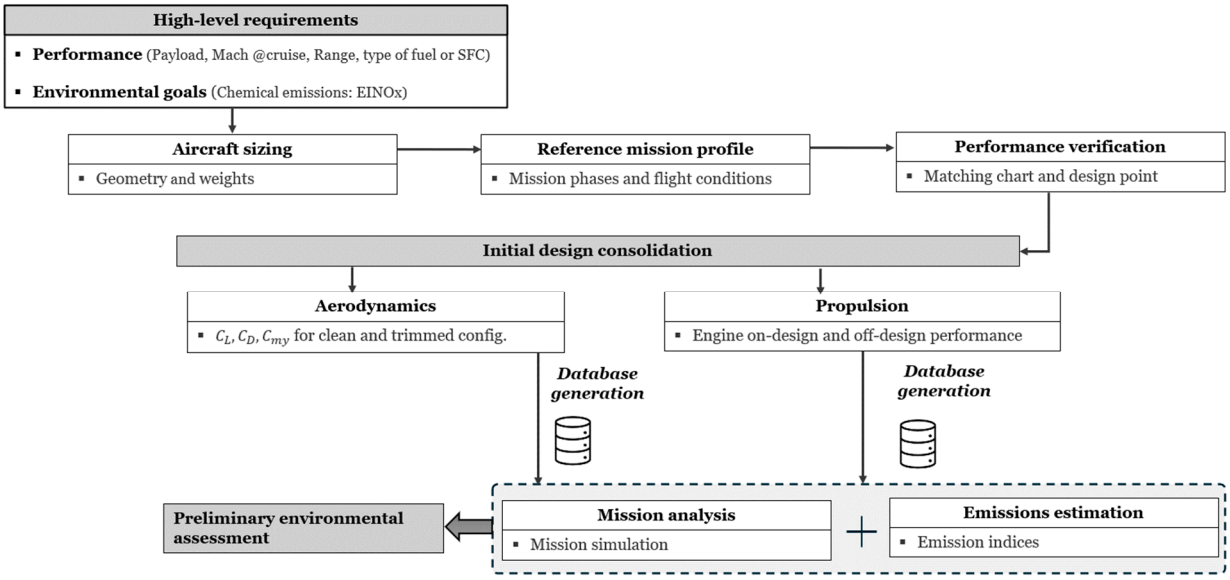

Figure 1. Multi-disciplinary approach underlying the overall design methodology.

On the other hand, to enable mission simulation and emission estimation, propulsive characterization is also required. Since propulsion modeling software tools are either unavailable, not easy to integrate, or not tailored for supersonic flight applications, and do not directly provide the necessary emission estimation data, a dedicated engine model was developed to address this gap. This model can perform both on-design and off-design analyses, considering various high-level requirements for supersonic aircraft, to propose the sizing of a specific engine for each of the developed concepts. Additionally, it generates a propulsion database with thrust and SFC values across different Mach numbers, altitudes, and throttle settings for mission simulation. The propulsive database can then be used to feed a multi-fidelity emission estimation model. In the case where proprietary propulsive characteristics such as pressure and temperature at the entrance of the combustion chamber are available, P3-T3-based correlation methods can be used to estimate the emission indices in any flight condition [36]. In the case where proprietary propulsive characteristics are not available, it is necessary to rely on already existing and certified engine technology for the LTO emissions and on simpler correlation methods, such as the Boeing Fuel Flow Method [29] where fuel flow is used as main parameter to scale the engines emissions along the trajectory. However, when evaluating case studies like the one dealt with in this study (i.e., supersonic speed and the use of biofuels) that move beyond the range of applicability of the original correlation methods, the mathematical formulations should be substituted with newly developed ones that are sensitive to Mach number and fuel type variations [30,37,38].

Finally, once the aerodynamic and propulsion databases are complete, mission simulation and environmental evaluation can proceed, using emission indices values to verify the environmental impact of the aircraft. It is worth noting that this method focuses on investigating possible solutions to reduce environmental impacts, primarily those related to aerodynamics and propulsion systems. Still, other aspects such as structural layout and characterization are also crucial for the design process. However, even if weight estimations and breakdowns that include structural basic computations are implemented, a detailed structural assessment is not carried out.

3. Rapid Aircraft Prototyping Tool: ASTRID-H 2.0

The overall design methodology outlined in Section 2 forms the theoretical foundation for the development of ASTRID-H 2.0. This tool was used to preliminarily size the Mach 1.5 case study described in Section 5. ASTRID is a proprietary tool developed by the research group which the authors belong to at the Polytechnic University of Turin. It has

evolved over the years to support the conceptual and preliminary design of aircraft, as well as the sizing and integration of subsystems, primarily for subsonic and low supersonic speeds [39]. ASTRID-H is an extension of this tool, specifically designed for high-speed vehicle applications. The latest version (2.0) addresses civil supersonic aircraft designs, covering supersonic speeds from Mach 2 to 5, and considers the impact of alternative fuels on aircraft design. The efforts towards improving ASTRID-H 2.0 have focused on revising the conceptual design process to achieve more accurate estimates of high-speed aircraft performance and preliminary evaluations of environmental requirements. The upgraded stratified structure, characterized by progressively increasing levels of fidelity, is depicted in Figure 2.

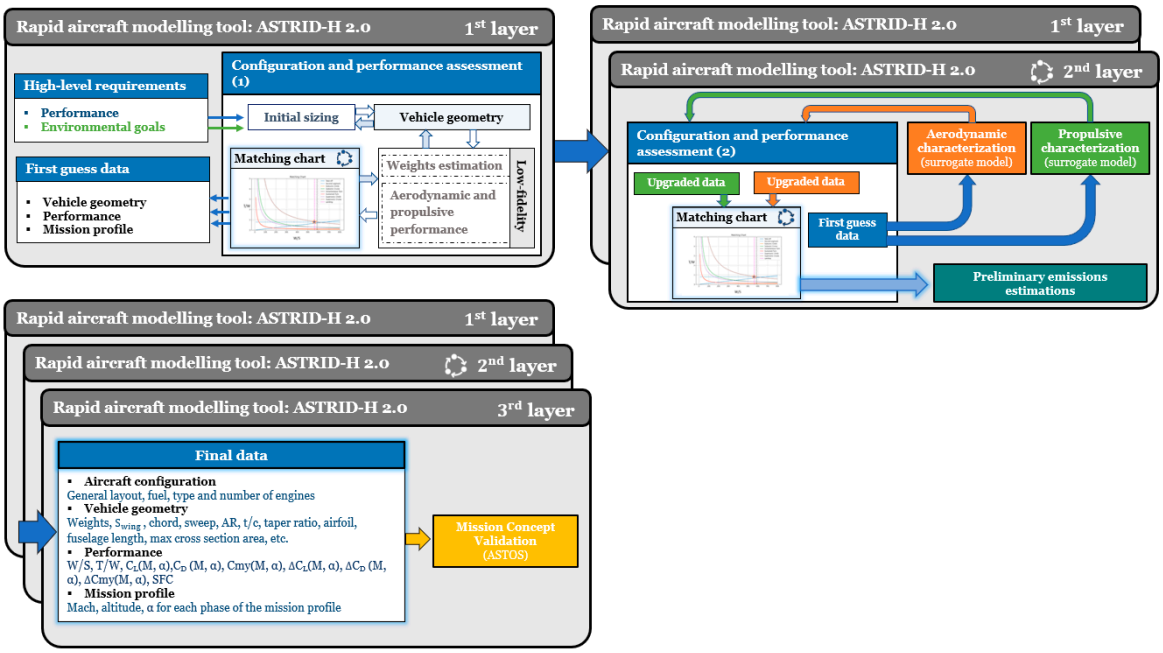

Figure 2. ASTRID H 2.0 tool structure.

The design process starts with the first layer, which includes conventional conceptual design steps to establish an initial aircraft layout and preliminary performance estimates using the matching chart tool. This is followed by a second layer with enhanced fidelity, refining the supersonic aircraft characterization through more accurate aerodynamic and propulsion modeling. Here, the proposed algorithms for the mixed-flow turbofan engine model were integrated, ensuring a certain level of adaptability for future updates. Then, the enhanced data are used to revise the initial matching chart outputs and finalize the aircraft configuration. Once this is complete, the necessary data for preliminary emission estimation are available. The third layer involves mission simulation to validate the design and consolidate the output data.

4. Propulsion System Modeling

An engine model for conceptual design must be flexible and adaptable to various requirements and design parameters. Different options to integrate engine modeling from the early stage of design may be employed depending on the desired level of fidelity. Statistical methods, based on tabulated engine performance data might be used to initially size the engine [40]. Then, for a more specific characterization, an analytical model can be developed using data from an existing engine, often a military one, to estimate missing parameters or propose redesigns [19,41]. Another option is to use dedicated software tools to define new propulsion systems. These tools can be tailored to specific objectives such as thermodynamic cycle analysis, performance prediction, weight estimation, as well as component sizing, and can be integrated with additional capabilities for component

analysis. For example, in [25], a new turbofan engine was designed for a conceptual supersonic business jet with a maximum cruise Mach number of 1.5. The NPSS code by NASA was used for the thermodynamic cycle analysis, followed by basic sizing and aerodynamic design. The same tool was also used in [11] to redesign a known engine for a Mach 1.4 supersonic business jet for environmental studies. In another study [42], the components of a new turbofan engine were preliminarily sized based on cycle and performance analysis using the GTlab framework [43] enhanced with knowledge-based methods for geometry and mass estimation of rubber aeroengines [44]. Additionally, in [45], a propulsion system was modeled for a conceptual supersonic transport aircraft with a passenger capacity of 200 and a cruise speed of Mach 3, comparing the performance of three engine configurations using GasTurb software, and was complemented by a cost analysis.

However, these tools are typically not accessible and were originally developed for subsonic applications or military supersonic aircraft, and later adapted for commercial supersonic aircraft studies. Therefore, in this section, an engine model is proposed that does not rely on external tools or proprietary data and allows for the definition of a new propulsion system directly tied to the high-level requirements of the aircraft. This model is fully replicable and can be integrated into multidisciplinary design processes, aiding in the conceptual design of more sustainable commercial supersonic airplanes. Figure 3 illustrates how propulsion system modeling was incorporated into the overall design methodology, enabling mission simulation and pollutant emissions estimation. After finalizing the aircraft layout, including the number of engines, geometric and installation constraints, as well as design conditions, like thrust-to-weight ratio (T/W) and flight conditions, propulsion system modeling can begin. From the propulsion section in Figure 3, the primary step is the one that substantially determines the performance of the propulsion system, that is, the selection of the engine thermodynamic cycle. For aircraft operating at supersonic cruise speeds up to Mach 3, turbojets and mixed-flow turbofans, frequently equipped with afterburners, have been the sole viable option in practical applications. However, innovative concepts like Turbine Bypass Engines (TBEs), Variable Cycle Engines (VCEs), Fan-on-Blade (Flade) engines, and Inverting Flow Valve (IFV) engines have also been explored [46]. Among these, VCEs could balance performance, economic, and environmental needs but may be too complex and costly. Considering performance, weight, and system complexity, mixed-flow turbofans are currently the most viable option, and hence, they were the focus of this study.

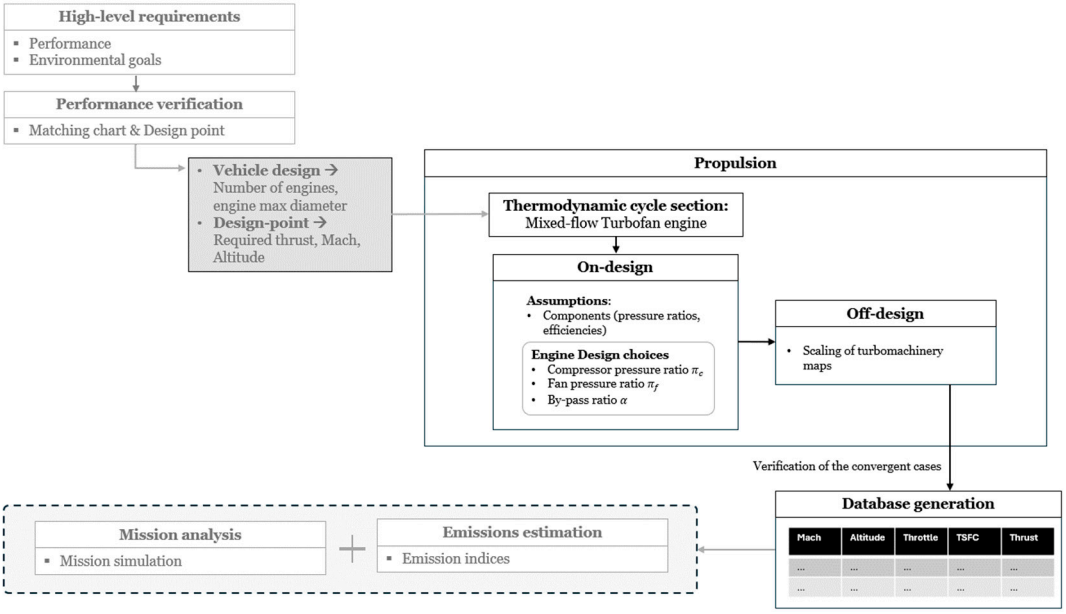

Figure 3. Propulsion system modeling process and integration in the overall design process.

The propulsion system schematics is presented in Figure 4. As already specified, the engine cycle is a mixed-flow turbofan and Figure 4 illustrates its architecture and components. The engine has two spools: a low-pressure spool, where a fan (F), a low-pressure compressor (cL), and a low-pressure turbine (tL) are installed, and a high-pressure spool, where a high-pressure compressor (cH) and a high-pressure turbine (tH) are mounted. The air mass flow rate is depicted by the dashed orange lines. The cold stream flowing through the fan and the hot stream from the core are mixed before the exhaust. The turbines are both cooled with bleed air fractions (ϵ_1, ϵ_2) extracted from the high-pressure compressor outlet (cH). The fuel mass flow rate is depicted by the dashed red line and finally, the power extraction from the two spools is depicted by the dashed green lines. Notably, the exhaust nozzle is a convergent–divergent nozzle with a variable exit area. The numbering of the engine stations is explained in Table 1, which specifies the inlet and outlet of each engine component. The engine cycle was modeled using Mattingly's method for estimating the performance of a mixed-flow, cooled, two-spool turbofan engine [47,48].

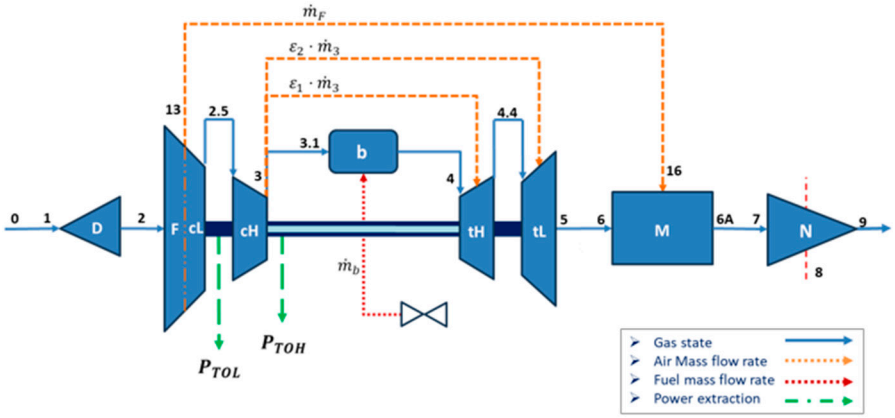

Figure 4. Mixed-flow turbofan engine schematic.

Table 1. Engine station numbering.

Engine Station Numbering	
0	Fan upstream or freestream
1	Inlet or diffuser entry
2	Inlet or diffuser exit, fan entry, low-pressure compressor entry
13	Fan exit
2.5	Low-pressure compressor exit, high-pressure compressor entry
3	High-pressure compressor exit
3.1	Burner entry
4	Burner exit
4.1	Nozzle vane entry Coolant mixer 1 entry
4.4	High-pressure turbine entry High-pressure turbine exit Modeled coolant mixer entry
4.5	Coolant mixer 2 exit Low-pressure turbine entry
5	Low-pressure turbine exit
6	Core stream mixer entry
16	Fan bypass stream mixer entry
6A	Mixer entry Afterburner entry
7	Afterburner exit Exhaust nozzle entry
8	Exhaust nozzle throat
9	Exhaust nozzle exit

The on-design (or parametric) analysis is the next step, which is conducted to choose the engine design parameters that meet the propulsion system requirements. At this stage, the engine geometry is not yet defined, allowing for trade studies to identify the optimal solution. Once the design parameters (π_c, π_f or α) are set, the engine design is fixed, and off-design analysis can be carried out. This involves scaling the turbomachinery maps, solving a set of engine balancing equations, and studying the engine's behavior across different throttle settings, flight Mach numbers, and altitudes, thereby obtaining the operating lines on the map components. The off-design analysis is performed iteratively, with the converged results organized into a propulsive database that represents the engine's performance envelope, which is then used for mission simulations.

The assumptions underlying the thermodynamic cycle modeling are summarized below:

- The flow is, on average, steady and one dimensional.
- The working fluid is modeled as a "half-ideal gas" using Variable Specific Heat (VSH).
- A reference fuel, $C_{12}H_{23}$ (JP-4), is adopted.
- The inlet is modeled according to MIL-E-5008B.
- Both turbines provide power to the installed accessories.
- The turbine is cooled by air fractions bled from the high-pressure compressor.
- The constant area mixer is adopted.

Next, the general equations used to determine the main properties of the engine components and calculate the gas state at each station for both the on-design and off-design analyses are described.

The first component is the inlet, which is assumed to be integrated into the engine. The military specification MIL-E-5008B [47] was adopted to estimate the variation in adiabatic efficiency η_R and total pressure ratio π_d with the flight Mach number M_0, as reported in Equations (1) and (2).

$$\pi_d = \pi_{d,max}\, \eta_R \tag{1}$$

$$\eta_R = \begin{cases} 1 & M_0 \leq 1 \\ 1 - 0.075(M_0 - 1)^{1.35} & 1 < M_0 \leq 5 \\ \frac{800}{M_0^4 + 935} & M_0 > 5 \end{cases} \tag{2}$$

The model allows us to evaluate the inlet performance of supersonic inlets with external compression. It assumes no pressure losses under subsonic conditions and estimates η_r for supersonic speeds by calculating the total pressure ratio as the product of the total pressure ratio across the shocks that occur at supersonic speeds, accounting for the increasing pressure drop as the flight Mach number rises.

The compressors are assumed to be adiabatic and, to account for the fact that compressors consist of multiple stages, the polytropic efficiency e_c (determined accordingly to the assumed technology level) is introduced in Equations (3) and (4) to calculate the compressors' pressure ratio π_c and temperature ratio τ_c.

$$\pi_c = \left(\frac{P_{t3}}{P_{t_2}}\right)^{e_c} \tag{3}$$

$$\tau_c = \pi_c^{\frac{\gamma-1}{\gamma e_c}} \tag{4}$$

A simplified model based on combustion efficiency was employed to estimate the combustor performance. By knowing the P_{t3}, h_{t3}, or T_{t3}, computed at the exit of the high-pressure compressor stage, and considering the lower heating value h_{PR} of the fuel, it is possible to define the combustion efficiency:

$$\eta_b = \frac{\dot{m}_4 h_{t4} - \dot{m}_3 h_{t3}}{\dot{m}_f h_{PR}} \tag{5}$$

In Equation (5), $\dot{m}_f$ is the fuel mass flow rate, $\dot{m}_3$ is the air mass flow upstream of the combustion chamber, and $\dot{m}_4$ is the sum of these rates. During on-design simulations, η_b is specified as a design parameter and is related to the level of technology. From the combustion efficiency, it is possible to calculate the fuel-to-air ratio:

$$f = \frac{\dot{m}_f}{\dot{m}_3} = \frac{C_p T_{t4} - C_p T_{t3}}{\eta_b h_{PR} - C_p T_{t3}} \tag{6}$$

where typically the Turbine Inlet Temperature (TIT) T_{t4} is known since it is a design parameter. Equation (6) assumes a calorically perfect gas. For a more general VSH gas model, it may not be used directly. Therefore, an iterative algorithm was employed to calculate f until convergence is reached, using a predefined tolerance. Finally, the pressure losses are considered constant, with the parameter π_b defined as

$$\pi_b = \frac{P_{t4}}{P_{t3}} \tag{7}$$

Similarly to the compressors, the turbines are assumed to be adiabatic and the pressure ratio π_t and temperature ratio τ_t are computed as follows:

$$\pi_t = \left(\frac{P_{t5}}{P_{t_4}}\right)^{1/e_t} \tag{8}$$

$$\tau_t = \pi_t^{\frac{\gamma-1}{\gamma(\frac{1}{e_t})}} \tag{9}$$

Since the turbines are cooled, the assumption of adiabatic flow seems to not be entirely accurate, but it can be considered acceptable for preliminary design purposes. The turbine is cooled by extracting a fraction of air from the compressor (before it enters the combustion chamber) and routing it through internal passages within the engine to cool various components. This bleed air is then released into the turbine section to provide cooling. The fraction of the total mass flow rate used for cooling (ϵ) in an aircraft engine varies depending on the specific engine design and operating conditions, but typically is a small percentage in the range of 1% to 6% of the total airflow. The exact fraction may vary based on factors such as the engine type, power settings, and environmental conditions. The precise fraction of air extracted from the compressors is estimated according to Equation (10):

$$\epsilon = \begin{cases} 0 & T_{t4} < 1332 \\ \frac{1.8\ T_{t4,\ max} - 2400}{16{,}000} & T_{t4} \geq 1332 \end{cases} \tag{10}$$

To increase the accuracy of the model, the mechanical power extraction of the turbine P_T may be included with the related efficiency η_{mP}. The general power balance equation for each shaft is then modified as follows:

$$\dot{W}_c = \dot{W}_t \eta_m + \frac{P_T}{\eta_{mP}} \tag{11}$$

where $\dot{W}_c$ and $\dot{W}_t$ are the work of the compressor and turbine and η_m is the mechanical efficiency.

Downstream of the low-pressure turbine is the mixer. Mixing the cold stream from the bypass with the hot stream from the core offers several advantages, especially for supersonic applications. Firstly, it can increase thrust if the total pressures in the core and bypass streams are similar, as this minimizes pressure loss during mixing. Secondly, the mixing can reduce noise during take-off by lowering the jet exhaust speed. Additionally, the mixer could be necessary when the use of afterburners or reheaters is being considered. However, a significant disadvantage of using mixers is the added weight they bring to the

system. For this reason, their inclusion is always carefully considered during the design of propulsion systems. Here, the mixer is modeled as an ideal mixer with a constant area and no wall friction. A set of balance equations is applied to the mixer's control volume, identified by its inlet and outlet stations, to determine its main parameters. From the perspective of mass conservation, it is possible to define the mixer bypass ratio, that is the ratio of the cold mass flow at the fan outlet and total mass flow at the mixer outlet:

$$\alpha' = \frac{\dot{m}_{16}}{\dot{m}_6} \tag{12}$$

By applying the energy balance equation, the mixer temperature ratio τ_M is calculated as

$$\tau_M = \frac{h_{t6A}}{h_{t6}} = \frac{1 + \alpha'(h_{t16} + h_{t6})}{1 + \alpha'} \tag{13}$$

where h_t is the total enthalpy. Then, the ideal mixer pressure ratio is calculated as

$$\pi_{M,ideal} = \frac{P_{6A}}{P_{t6}} = (1 + \alpha)\sqrt{\tau_M}\frac{A_6}{A_{6A}}\frac{MFP(M_6, T_{t6},\ f_6)}{MFP(M_{6A}, T_{t6A},\ f_{6A})} \tag{14}$$

The mathematical relationships used to calculate the parameters in Equation (14) are provided below. The fuel-to-air ratio at the mixer outlet is given by

$$f_{6A} = \frac{f_6}{1 + \alpha'} \tag{15}$$

MFP is the Mass Flow rate Parameter, which is defined as

$$MFP = \frac{\dot{m}\ \sqrt{T_t}}{P_t\ A} \tag{16}$$

The evaluation of the area at the mixer outlet A_{6A} assumes that the mixer has constant area; then, the outlet area is equal to the sum of inlet ones A_{16} and A_6. Using the Kutta condition that imposes $P_{t16} = P_{t6}$, the mixer inlet area ratio is computed as

$$\frac{A_{16}}{A_6} = \alpha'\sqrt{\frac{T_{t16}}{T_{t6}}}\frac{P_{t6}}{P_{t16}}\frac{MFP(M_6, T_{t6},\ f_6)}{MFP(M_{16}, T_{t16},\ f_{16})} \tag{17}$$

In Equation (14), the mixer inlet Mach number M_6 is assumed to be known as it is a design parameter. Using the Kutta condition and applying the isentropic formula, the Mach number at the fan outlet M_{16} is calculated as

$$M_{16} = \frac{2}{\gamma - 1}\left[\frac{P_{t16}}{P_{t6}}\left(1 + \frac{\gamma_{16} - 1}{\gamma_{16}}M_6^2\right)^{\frac{\gamma_6 - 1}{\gamma_6}}\right] \tag{18}$$

The Mach number at the mixer outlet M_{6A} is calculated from the momentum equation involving M_6 and M_{16}:

$$\sqrt{\frac{R_{6A}T_{6A}}{\gamma_{6A}}}\frac{1 + \gamma_{6A}M_{6A}^2}{M_{6A}} = \sqrt{\frac{R_6T_6}{\gamma_6}}\frac{\left(1 + \gamma_6M_6^2\right) + A_{16}/A_6\left(1 + \gamma_{16}M_{16}^2\right)}{M_6(1 + \alpha')} \tag{19}$$

The right-hand side of Equation (19) remains constant and is derived from previous computations. Equation (19) is inherently nonlinear, with the variable of interest being M_{6A}. Once solved, the determined value of M_{6A} is subsequently employed in the calculation of $\pi_{M,ideal}$ in Equation (14). To account for pressure losses, it is possible to calculate the mixer pressure ratio as

$$\pi_M = \pi_{M,ideal}\ \pi_{M,\ max} \tag{20}$$

where $\pi_{M,\,max}$ represents an estimation of the losses due to friction and it is generally assumed to be around 0.97. Ultimately, it is important to ensure that the Kutta condition is satisfied, which means that

$$\frac{P_{t16}}{P_{t6}} = \frac{\pi_f}{\pi_{cL}\pi_{cH}\pi_b\pi_{tH}\pi_{tL}} \cong 1 \tag{21}$$

A potential strategy is to select the appropriate value of π_f during the parametric analysis to satisfy Equation (21).

With the values of $\pi_{M,max}$ and M_6 known, Equations (1) to (21) can be used to analyze the thermodynamics and determine the mixer areas for both the on-design and appropriately reformulated off-design conditions.

Ultimately, the nozzle is modeled as an adiabatic convergent–divergent duct with a variable geometry, assuming isentropic flow. The throat and exit area are adjusted to ensure the adaptation condition, so that the exit pressure matches the ambient pressure ($P_9 = P_0$). Specifically, if the flow is subsonic, the nozzle behaves as a convergent duct. Conversely, if the throat is at critical conditions with $M_8 = 1$, the throat area is adapted to avoid chocking using the MFP:

$$A_8 = \frac{\dot{m}_8\sqrt{T_{t8}}}{P_{t8}MFP(M_8, T_{t8}, f_8)} \tag{22}$$

Then, the exit area is adjusted computing the exit Mach number M_9 using isentropic flow relationships, knowing the total pressure P_{t9} and the static pressure from $P_9 = P_0$. These relationships form the foundation for engine characterization in both on-design and off-design analyses. However, moving towards off-design simulations, additional assumptions are required:

- The flow areas are constant at stations 4, 4.5, 6, 16, and 6A.
- The exit area of the nozzle (A_9) is adjustable to maintain the exit pressure ratio of the exhaust equal to the external one ($P_9 = P_0$) or to a selected ratio P_9/P_0.
- The area of station 8 remains constant at its reference value.
- The map scaling procedure is adopted.

The matrix iteration method, also known as the component matching method, is employed for off-design simulations. This method uses the balancing equations of power and corrected mass flow rate. For dual-spool mixed-flow engines, the state vector in Equation (23) follows the approach in [49], although the present method is expected to also align with that in [50,51].

$$\overline{X} = \{\pi_{cL},\ \pi_{cH},\ \pi_{tL}, \pi_{tH},\ N_{cL,}\ N_{cH}\} \tag{23}$$

The function vector requires at least six balancing equations: low-pressure spool power balance, high-pressure spool power balance, the Kutta condition, congruence of the corrected mass flow rate between the high-pressure compressor and the high-pressure turbine, corrected mass flow rate between the high-pressure compressor and the low-pressure turbine, corrected mass flow between the mass flow rate at the inlet of the nozzle and the low-pressure compressor. In off-design analyses, the state vector represents the engine's dependent variables.

To find a solution, independent variables such as flight Mach number M_0, external pressure P_0, or temperature T_0, and TIT must be specified to simulate the off-design conditions. However, deviations from the design point can cause imbalances in the equations, so the state vector needs to be adjusted to satisfy these parameters. Essentially, the compressor and turbine operating conditions must be regulated to meet new operating conditions while adhering to mixer and nozzle constraints. Therefore, the Newton–Raphson method is used to compute this updated state vector.

The results of this calculation are then used to interpolate the operating points on the scaled turbomachinery maps, obtaining the working lines of the components. At this

stage, the conceptual design of the entire propulsion system is complete, allowing for off-design simulations. By adjusting the flight conditions and throttle settings, all flight mission phases can be examined. Thus, the resulting database can be used for mission simulation and emission estimation.

4.1. Gas Model: Variable Specific Heat (VSH)

The thermodynamic state of the gas is modeled by considering the specific heat at constant pressure C_p as a variable with temperature and is calculated at each station of the engine. This approach allows for a more accurate estimation of engine performance, as shown in Figure 5 [52].

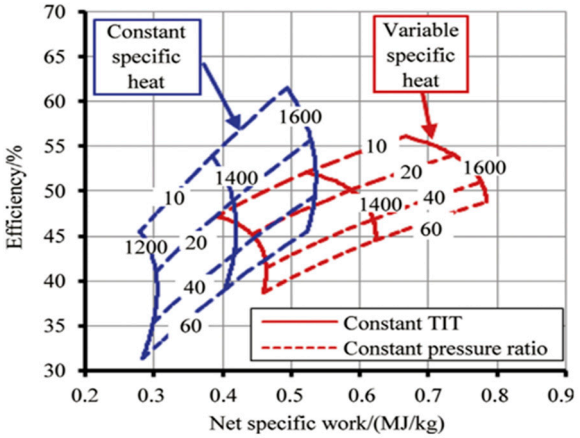

Figure 5. Comparison between constant and variable specific heat performance calculation [52].

Therefore, the working fluid is modeled as a half-ideal perfect gas, which implies that the gas obeys the following properties:

$$C_p = f(T)\ C_p \neq f(P) \tag{24}$$

So, the specific heat at constant pressure is defined by

$$C_p = \left(\frac{\partial h}{\partial T}\right)_{P=const} \tag{25}$$

In general, the hypothesis of the half-ideal gas model is valid for temperatures above 200 K up to 2220 K for air and air–fuel mixtures. The final expression for enthalpy can be obtained from previous equation:

$$h(T) = \int_{T_{ref}}^{T} C_p(T)dT \tag{26}$$

where, T_{ref} is the reference temperature, which can be selected arbitrarily. To evaluate enthalpy values, it is essential to identify C_p values. The most common method for doing this is by using the algorithm proposed by Gordon and McBride [53]. This algorithm, which forms the basis of the CEA run software [54], involves the use of a polynomial with seven terms. However, for consistency with the methodology used in this work, the Mattingly model [55] was followed, which uses a polynomial of the seventh degree.

$$C_P = A_0 + A_1T + A_2T^2 + A_3T^3 + A_4T^4 + A_5T^5 + A_6T^6 + A_7T^7 \tag{27}$$

The polynomial coefficients that were considered are listed in Table 2.

Table 2. Constants for air and combustion product with hydrocarbons [55].

	Air Alone	Combustion Products of $(CH_2)_n$ Fuels
A0	2.50×10^{-1}	7.38×10^{-2}
A1	-5.15×10^{-5}	1.22×10^{-3}
A2	6.55×10^{-8}	-1.38×10^{-6}
A3	-6.72×10^{-12}	9.97×10^{-10}
A4	-1.51×10^{-14}	-4.20×10^{-13}
A5	7.62×10^{-18}	1.02×10^{-16}
A6	-1.45×10^{-21}	-1.33×10^{-20}
A7	1.01×10^{-25}	7.26×10^{-25}
$\mathbf{h_{ref}}$ **[Btu/lbm]**	−1.75	30.6
$\boldsymbol{\phi_{ref}}$ **[Btu/(lbm °R)]**	4.54×10^{-2}	6.48×10^{-1}

It is now possible to calculate, for a mixture of air and a generic hydrocarbon $(CH_2)_n$ with a given fuel-to-air ratio f, the specific heat of the fuel and air mixture:

$$C_p = \frac{C_{p,air} + fC_{p,prod}}{1+f} \tag{28}$$

Other important quantities to evaluate for the half-ideal gas model include enthalpy h, the entropy function ϕ, and the reduced pressure P_r. The respective polynomial functions are as follows:

$$h = h_{ref} + A_0 T + \frac{A_1}{2}T^2 + \frac{A_2}{3}T^3 + \frac{A_3}{4}T^4 + \frac{A_4}{5}T^5 + \frac{A_5}{6}T^6 + \frac{A_6}{7}T^7 + \frac{A_7}{8}T^8 \tag{29}$$

$$\phi = \phi_{ref} + A_0\, ln(T) + \mathrm{A}_1 T + \frac{A_2}{2}T^2 + \frac{A_3}{3}T^3 + \frac{A_4}{4}T^4 + \frac{A_5}{5}T^5 + \frac{A_6}{6}T^6 + \frac{A_7}{7}T^7 \tag{30}$$

$$P_r = e^{\frac{\phi - \phi_{ref}}{R}} \tag{31}$$

For an air–gas mixture,

$$h = \frac{h_{air} + fh_{prod}}{1+f} \tag{32}$$

$$\phi = \frac{\phi_{air} + f\phi_{prod}}{1+f} \tag{33}$$

The reduced pressure is a useful parameter for modeling engine components; in fact, it is related to the OPR (Overall Pressure Ratio) π_c as follows:

$$\pi_c = \left(\frac{Prt_3}{Prt2}\right)^{e_c} \tag{34}$$

The mathematical relationships described above were implemented in a dedicated routine (called FAIR) integrated in the propulsion model. In particular, it allows for the evaluation of the entire gas state using one of the following inputs: temperature (T), enthalpy (h), or reduced pressure (P_r). Also, the fuel-to-air ratio (f) of the mixture must be given, otherwise, if the gas is air, it is possible to set it equal to zero. The outputs include the following:

- R: the universal gas constant of the mixture;
- C_p: the constant pressure specific heat of the mixture;
- γ: the ratio of the constant specific heat at constant pressure over the constant specific heat at constant volume of the mixture;
- a: the speed of sound of the mixture;
- T: the temperature of the mixture (if unknown);
- h: the enthalpy of the mixture (if unknown);

- ϕ: the entropy function;
- s: the entropy of the mixture;
- P_r: the reduced pressure of the mixture (if unknown).

In cases where enthalpy or pressure is the input, a nonlinear system must be solved to obtain the temperature and other quantities. The solution of the system can be obtained using the Newton–Raphson method with a selected tolerance of 10^{-10}. The routine was validated using the data provided in [55].

Figure 6 visualizes how C_p varies with respect to temperature, given a fuel-to-air ratio from 0 to stoichiometric, using the FAIR function.

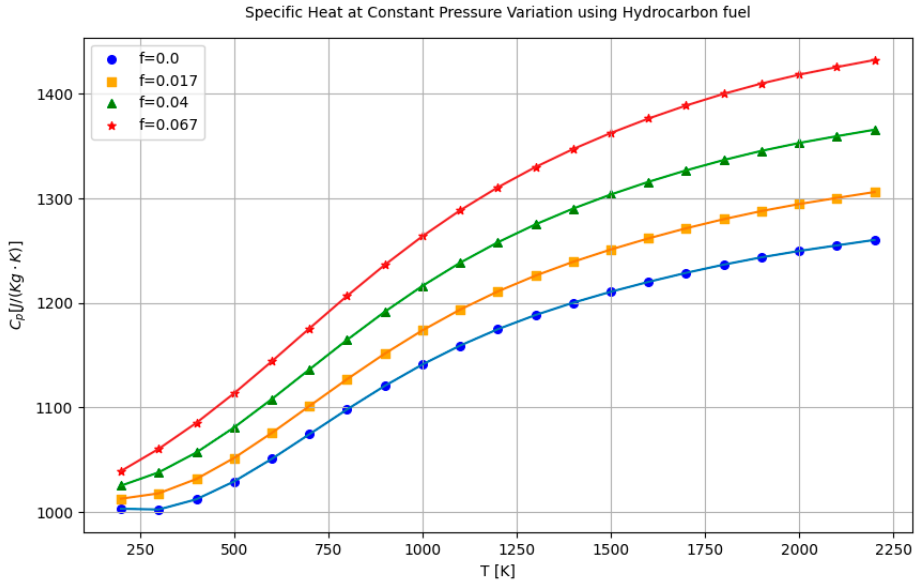

Figure 6. Specific heat variation as a function of temperature for different hydrocarbon fuel–air ratios.

This gas model can be used for different hydrocarbons, including drop-in biofuels, and has the potential to include hydrogen by updating the model and adapting the coefficients of the 7th degree polynomial for non-hydrocarbon fuels. This feature makes the proposed engine model adaptable to expand its applicability to a broader range of fuels, making it suitable to study sustainable supersonic aircraft concepts.

4.2. Parametric Analysis

Parametric cycle analysis, also known as on-design analysis, aims to correlate performance parameters, such as thrust and thrust-specific fuel consumption, with engine design choices (e.g., compressor and fan pressure ratios, BPR), design limitations (e.g., burner exit temperature, compressor exit pressure), and flight conditions (e.g., Mach number, ambient temperature). The method applied relies on [47,48,55] and the engine model used was described in Section 4, neglecting turbine cooling and power extraction. The input variables, which are the independent variables of the analysis, are reported in Table 3.

Table 3. Input variables for parametric cycle analysis for a mixed-flow, two-spool, turbofan engine.

Parametric Cycle Analysis (Input Variables)	
Flight parameters	M_0, T_0, P_0
Gas properties	γ, C_p
Fuel heating value	h_{PR}
Components (pressure ratios, efficiencies)	π_b, $\pi_{d_{max}}$, $\pi_{M_{max}}$, π_{AB}, π_n, η_b, η_{mL}, η_{mH}, e_f, e_{CL}, e_{CH}, e_{TH}, e_{TL}
Design choices	π_{CH}, π_{CL}, α, T_{t4}, T_{t7}, M_5, P_9/P_0

The inputs for the flight parameters were provided assuming the Top of Climb (TOC) as the design condition, which was set as the point at which the ascent to cruise altitude is completed. The analysis was performed for concepts with different design Mach numbers, defining a design space ranging from Mach 1.5 up to 3. In Table 4, the main inputs are reported, assuming technology level IV for the pressure ratios and efficiencies [47].

Table 4. Inputs for parametric cycle analysis.

Parametric Cycle Analysis Inputs		
Parameter	**Symbol**	**Value**
Inlet pressure ratio	$\pi_{d_{max}}$	0.995
Burner pressure ratio	π_b	0.96
Nozzle pressure ratio	π_n	0.98
Mixer pressure ratio	π_{Mmax}	0.96
Burner efficiency	η_b	0.995
Mechanical efficiency LP spool	η_{mL}	0.99
Mechanical efficiency HP spool	η_{mH}	0.99
Fan polytropic efficiency	e_f	0.89
LP compressor polytropic efficiency	e_{CL}	0.9
HP compressor polytropic efficiency	e_{CH}	0.9
HP turbine polytropic efficiency	e_{TH}	0.89
LP turbine polytropic efficiency	e_{TL}	0.89
Max turbine inlet temperature (TIT)	$T_{t4,max}$	2000 K
Afterburner exit temperature	T_{t7}	2200 K
Pressure ratio at nozzle exit	P_9/P_0	1.00
Mixer inlet Mach number	M_6	0.5
Fuel heating value	h_{PR}	43.260 MJ/Kg

The gas properties were calculated at each engine station using the VSH model described in the previous section, considering a conventional hydrocarbon as the fuel. The nozzle was assumed to be adapted for the design condition; hence, the pressure ratio between the pressure at the nozzle exit and the ambient pressure was set equal to 1.

Solving the equations for each stage of the engine, the parametric cycle analysis yielded an estimation of the overall engine performance. Specifically, the uninstalled specific thrust was calculated as

$$\frac{F}{\dot{m}_0} = V_0\left\{\left[\left(1+f_0-\frac{1}{1+\alpha}\right)\frac{V_9}{V_0}-1\right]+\left[\left(1+f_0-\frac{1}{1+\alpha}\right)\frac{R_{AB}}{R_c}\frac{V_0}{V_9}\frac{T_9}{T_0}\frac{(1-P_0/P_9)}{\gamma_c M_0^2}\right]\right\} \tag{35}$$

The uninstalled specific fuel consumption indicated as S was

$$S = \frac{f_0}{\left(\frac{F}{\dot{m}_0}\right)} \tag{36}$$

The parametric analysis was performed with varying engine design parameters (π_c and π_f or α) within the proper ranges for each supersonic concept flying at different Mach numbers. Figure 7 shows the results, represented by the carpet plots obtained by fixing the payload, range, and fuel at an altitude of 16,000 m and varying the cruise Mach number; the plots illustrate the variation in specific thrust and specific fuel consumption for different values of π_c and π_f. Once the required performance for the specific design conditions was determined, this analysis was used to select the point on the plot that corresponded to the engine design parameters where the specific thrust and fuel consumption met the desired specifications.

However, this analysis can be also useful to identify possible design limitations related to the adoption of a mixed-flow turbofan in the selected range of supersonic speeds.

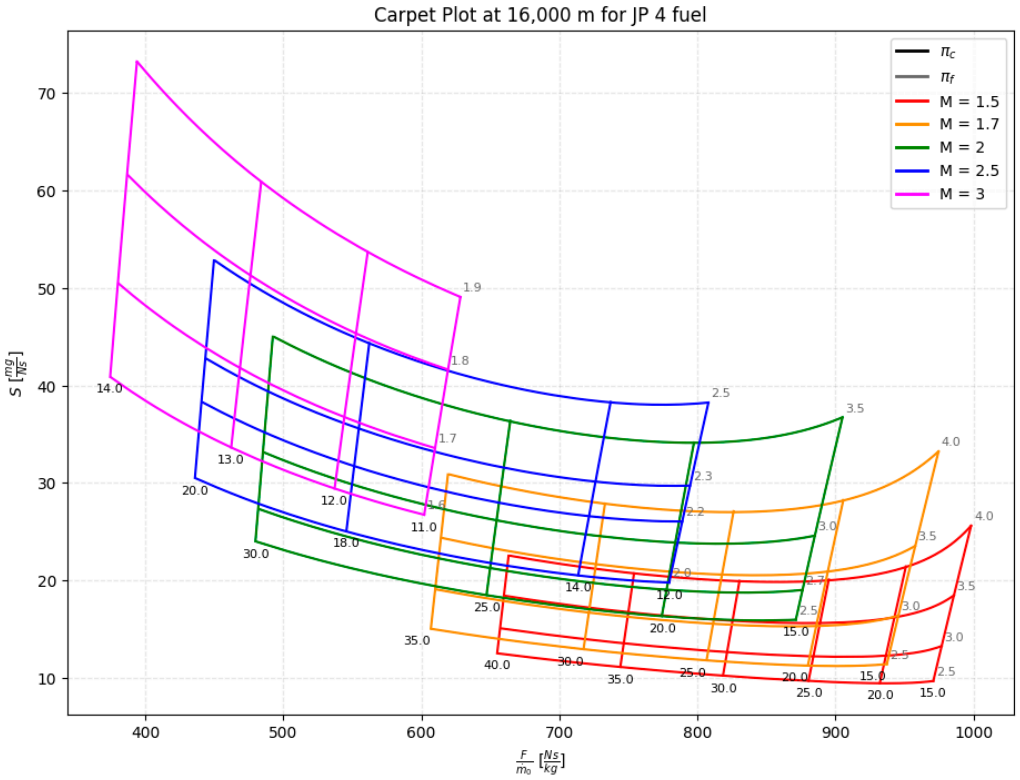

Figure 7. Parametric analysis: carpet plot for different cruise Mach numbers from 1.5 to 3.

Based on these carpet plots, the ranges of the compression ratio π_c and fan compression π_f were evaluated at each Mach number, as shown in Figure 8, considering both potential algorithm limitations and technological constraints. Therefore, a preliminary comparison was made with data from similar studies found in the literature. For the Mach 1.5 case, and with reference to the results in [11,19,25], the values appear to be consistent. Indeed, for aircraft configurations with cruise Mach numbers ranging from 1.4 to 1.6 at an altitude of 16 km, the value of π_c, also indicated as the OPR, under different design conditions can vary from 22 to 38, while the π_f value ranges from 5 to 2. When the cruise Mach number increases, a sensible decrease in π_c can be observed. A similar trend could also be attributed to limitations of the implemented algorithm, which does not guarantee convergence when the Mach number increases over large ranges of π_c and π_f. However, there is also a possible physical explanation, since at high Mach numbers, the air entering the compressor is already hot due to ram compression in the inlet. This hot air becomes even hotter as it is compressed, and if the π_c is too high, the air will exceed the metallurgical temperature limits of the compressor [45]. This trend was confirmed in other studies on engines for aircraft cruising at high Mach numbers, typically above Mach 2.5. One potential solution is to use a precooler, a heat exchanger that keeps the compressor and fan temperatures within safe structural limits while also pre-heating the fuel [56]. However, when a precooler is not used, such as in [45], π_c significantly decreases, reaching a value of 7.38, with a π_f value of 1.26.

One of the main challenges in supersonic aircraft engine design is selecting the optimal BPR (or α). Therefore, an analysis was conducted that also considered variations in this parameter. Typically, a high BPR is preferred for reduced noise during take-off and landing, while a low or zero BPR is better for supersonic cruising. The compromise is to use an intermediate BPR that balances both needs within a fixed cycle [19]. However, these assumptions are valid for not too high Mach numbers. The BPR values based on the π_c and π_f intervals considered in Figure 8 are presented in Figure 9 for the different Mach numbers.

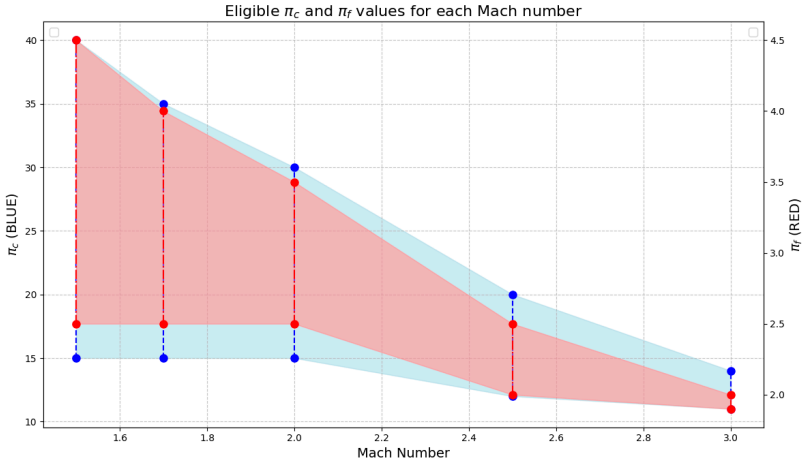

Figure 8. Parametric analysis: π_c and π_f variations with Mach number.

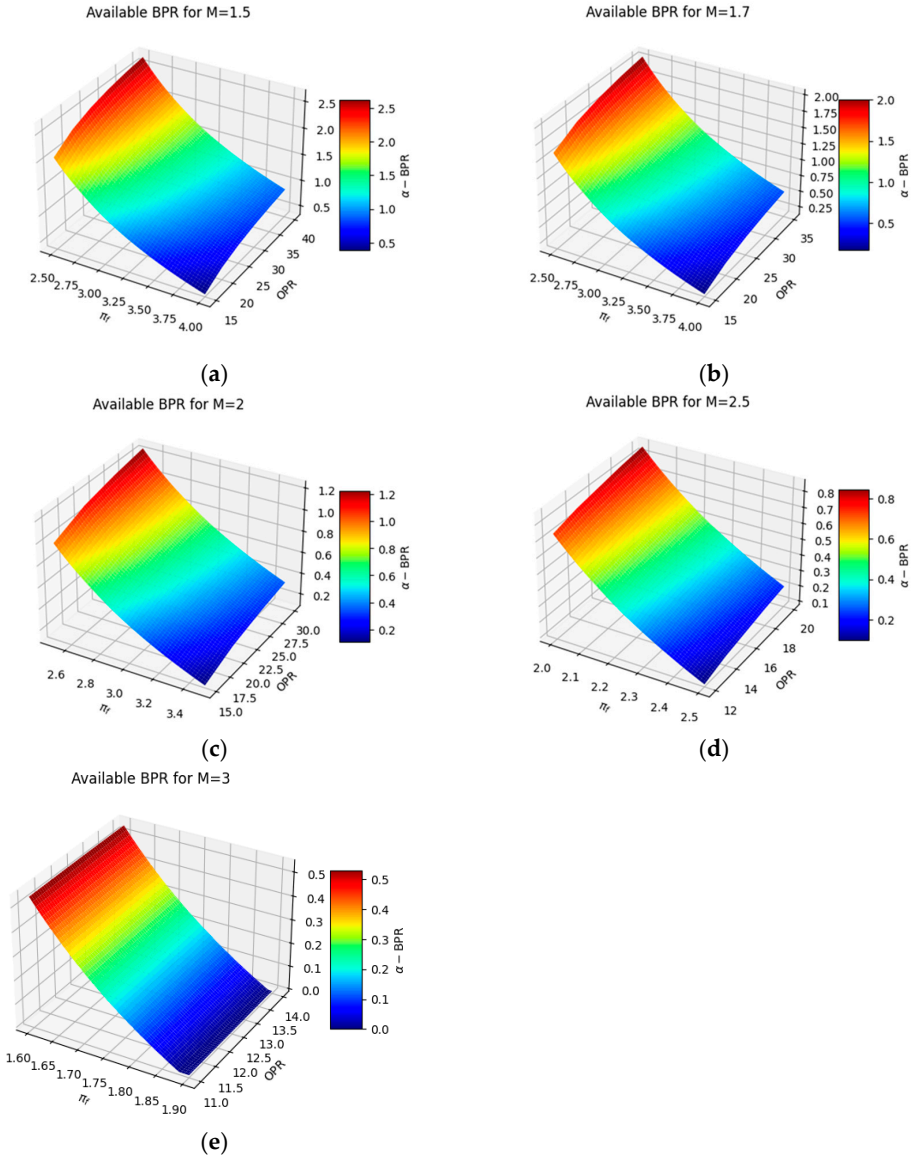

Figure 9. Parametric analysis: BPR variation diagram for (**a**) Mach 1.5; (**b**) Mach 1.7; (**c**) Mach 2; (**d**) Mach 2.5; (**e**) Mach 3.

The BPR varied between 0 (Turbojet) to 2.5 in lower speed cases. Considering the relationship between BPR, OPR, and π_f, increasing the BPR causes a very significant decrease in uninstalled thrust and a moderate decrease in S. As expected, the BPR ranges also narrowed as the Mach number increased; thus, the previously mentioned effect was smaller. For Mach values above 2.5, the design range became considerably restricted, as seen in Figure 8, and as a result, the allowable BPR values, already intrinsically low, were also reduced.

These results are further supported by the literature. Considering [11,19,25], the BPR can vary from 0.3 to 1.6 for aircraft cruising at Mach 1.5, but as the Mach number increases beyond 2.5, the trend is to move towards a zero BPR [45]. Indeed, from this speed on, it is advisable to change the type of technology and consider a Variable Cycle Engine (VCE) or ramjet [57], which are potentially attractive for aircraft which have to fulfil a mix of subsonic and supersonic missions.

4.3. Emissions Modeling

As the fuel flow is one of the key output parameters of this model, it can be exploited to run emission estimations using fuel-flow methods. They were developed based on the P3-T3 method, but with the objective of only using nonproprietary engine information, even at the cost of prediction accuracy. The main parameter considered by these prediction methods is the fuel flow, which represents the engine power setting and is publicly available. In addition, these methods take into account the effect of ambient pressure and temperature, humidity, and Mach number. Three fuel-flow methods are presented in the literature: the Boeing fuel-flow method 2 (BFFM2) [29] and its applications [58,59] and the sustainable supersonic fuel-flow method [30]. This family of methods can be very useful for a preliminary estimation of the emissions even if the achievable accuracy is lower than those attainable from the P3-T3 formulas.

Specifically, the $EINOx_{FL}$ is derived from a correction of the EINOxSL. However, for the BFFM2, this correction is performed based on the profiles of environmental conditions, the fuel flow profile Wf, and the humidity factor H. Unlike the P3T3 method, the BFFM2 involves an additional intermediate fitting step for the fuel flow parameter. To derive this parameter under SL conditions from that under FL conditions, a mathematical formulation is provided which includes the Mach number. Although the fuel flow parameter is not directly included in the final mathematical formula of the method used for evaluating EINOxFL, it serves as the parameter based on which, the EINOxSL values are plotted and interpolated. These interpolated values are then used for environmental correction, leading to EINOxFL. The complete procedure for applying the original BFFM2 can be summarized in the following steps.

As a first step, it is necessary to derive the fuel flow values at sea level corresponding to the four throttle settings prescribed by ICAO for the Landing Take-Off (LTO) cycle by applying the following correction to the fuel flow values in FL conditions.

$$w_{fSL} = w_{fFL} \frac{\theta_{amb}^{a}}{\delta_{amb}^{b}} \exp\left(cM^{d}\right) \tag{37}$$

$$\theta_{amb} = T_{amb}[K]/288.15 \tag{38}$$

$$\delta_{amb} = p_{amb}[Pa]/101,325 \tag{39}$$

It is possible to use exponential coefficients specifically tailored for the engine under study, although the original formulation of the method prescribes the following values: a = 3.8, b = 1, c = 0.2, and d = 2.

The $EINO_{xSL}$ values must be obtained from the ICAO Aircraft Engine Emissions Databank or estimated using appropriate modeling software. These values must then be curve-fitted as a function of the corrected fuel flow under SL conditions that was obtained

in the previous step (W_{fSL}). Once $EINO_{xSL}$ is determined, it is possible to estimate $EINO_{xFL}$ using the following formula:

$$EINO_{xFL} = EINO_{xSL}\left(\frac{\delta^{d}_{amb}}{\theta^{e}_{amb}}\right)^{f}\exp(H) \quad (40)$$

Similar to the P3T3 method, it is possible to use exponent coefficients specifically tailored for the engine under study, although the original formulation of the method prescribes the following values: d = 1.02, e = 3.3, and f = 0.5. H is the humidity factor that was previously introduced for the P3T3 method. Please note that, despite the BFFM2 appearing as a direct method, it is actually a ratio method because the parameters delta (δ) and theta (θ) represent ratios between environmental conditions at varying altitudes and those under SL standard conditions.

The main obstacle to the application of the approach suggested in this section, and of correlation methods in general, is the unavailability of LTO emissions data for newly developed and not-yet-certified engines. To temporarily overcome this problem (e.g., while waiting for high fidelity simulations to be available), the authors suggest using the main engine characteristics as filtering criteria for the ICAO Aircraft Engine Emissions Databank [60] to sort out the most similar engine technology available and to use the available data for LTO as a starting point. Then, as soon as more engine data are available, 0D chemical-kinetic simulations can be run for LTO conditions and the reference data are superseded.

5. Case Study: Mach 1.5

To derive all the necessary parameters for defining the propulsion system, the complete design methodology was applied to size a low-boom supersonic business jet cruising at Mach 1.5. This case study was chosen due to the significant interest in future low-boom concepts for business jet applications and related propulsion systems. The high-level requirements are presented in Table 5.

Table 5. Mach 1.5 aircraft requirements.

Aircraft High-Level Requirements	
Parameter	**Value**
Payload	1320 kg
Mach @cruise	1.5
Range	$\geq$ 3500 km
Sonic boom	$\Delta p_{max,\ cruise} < 1.5$ psf
Fuel	Biofuel

The aircraft shall cruise at Mach 1.5, accommodate up to 12 passengers, and have a range of up to 3500 km. To foster environmental sustainability, two additional requirements were added. The first was to minimize the near-field pressure signature to reduce the intensity of the sonic boom, while the second was to use 100% biofuel. The matching chart obtained using the ASTRID-H 2.0 tool is reported in Figure 10.

The performance requirements for a reference mission profile for supersonic aircraft were verified, leading to the determination of the design point in terms of the thrust-to-weight ratio (T/W) and wing loading (W/S_w, where S_w is the wing surface) from which the aircraft geometrical parameters and weights were determined. The main design data are reported in Table 6, including the Maximum Take-Off Weight (MTOW), which is the weight of the aircraft at take-off, and the Operating Empty Weight (OEW), which is the weight of the aircraft without payload and fuel.

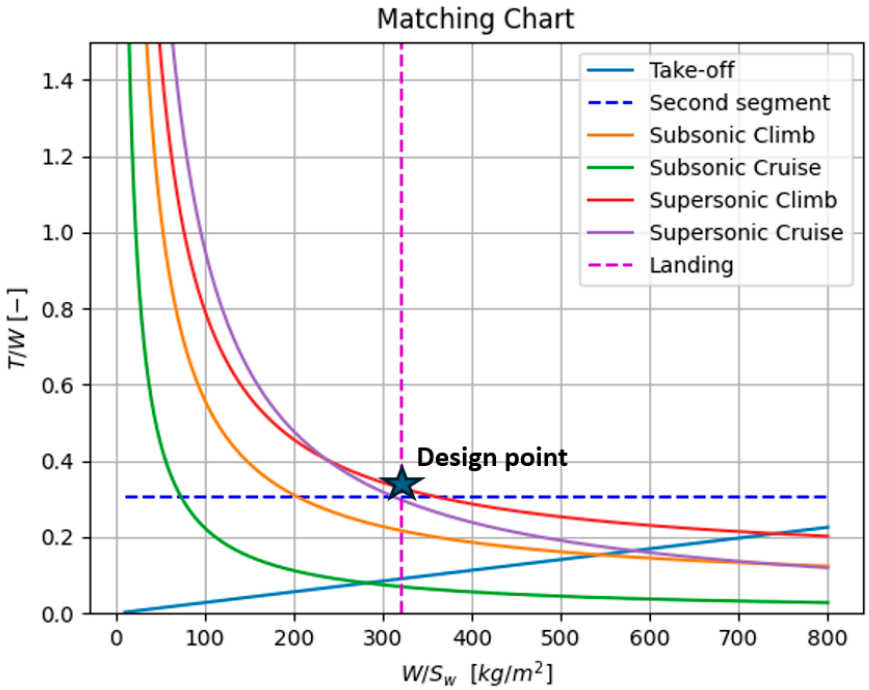

Figure 10. ASTRID-H 2.0 matching chart and design point.

Table 6. Mach 1.5 design data.

Design Data	
Parameter	**Value**
T/W	0.32
W/S_w	≅320 kg/m^2
MTOW	39,283 kg
OEW	19,048 kg
S_w	112 m^2
Length	44 m
Wingspan	14 m

The final CAD model of the aircraft is presented in Figure 11. To satisfy the low-boom requirement, the design was derived from the NASA X-59 QueSST [61], featuring a long, narrow airframe and canards to prevent shock waves from coalescing, ensuring a favorable far-field pressure distribution [62]. To accommodate 12 passengers and a crew of three (two pilots and one flight attendant), the central fuselage was enlarged with a seat pitch of 1.4 m. Two engines were considered for the propulsive powerplant, which was relocated from its original position under the vertical stabilizer at the tail to the wings. Propulsion system requirements were derived for the reference aircraft configuration based on the design loop results and are presented in Table 7. The required thrust was calculated from the thrust-to-weight ratio (T/W) at the design point (Table 6), which refers to the total required thrust. As mentioned earlier, two turbofan engines were considered; therefore, each engine requires approximately 62 kN of thrust, conservatively considering the MTOW in this flight phase at an altitude of about 15 km. Additionally, a constraint was applied to the inlet diameter to minimize drag from the engine nacelle. In this work, the inlet area was determined assuming that the Mach number at the intake was equal to 1.5. Because of this, knowing the mass flow, it is possible to obtain the area and, as consequence, the inlet diameter using the MFP equation (Equation (16)).

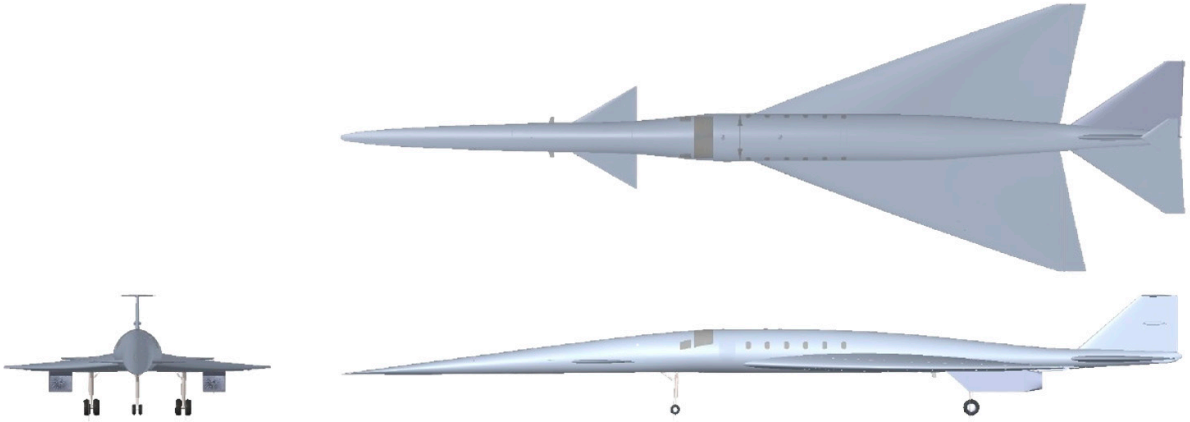

Figure 11. CAD model of the aircraft.

Table 7. Propulsion system requirements.

Propulsion System Requirements	
Parameter	**Value**
Number of engines	2
Inlet diameter	1.10 m
Mach @on-design	1.5
Altitude @on-design	16 km
Required Thrust @on-design	$\geq$62 kN

5.1. On-Design Analysis

Parametric cycle analysis was performed considering the propulsion system requirements in Table 7, and the carpet plot in Figure 12 was obtained.

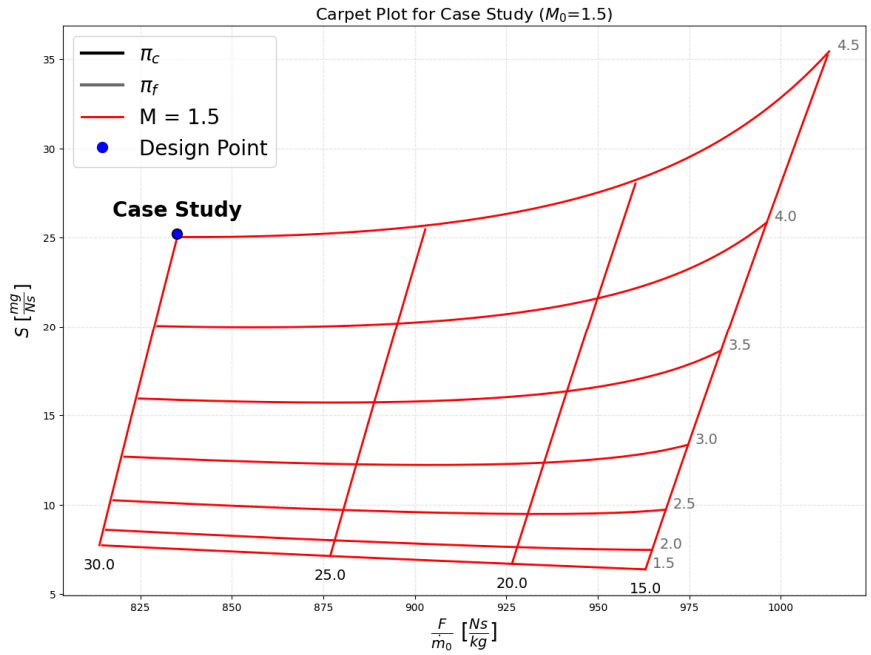

Figure 12. On-design carpet plot for Mach 1.5 case study.

The final mixed-flow turbofan design parameters are reported in Table 8. To satisfy the thrust requirement accounting for the airflow rate constraint, the point with the highest π_c equal to 30 was selected. Simultaneously, to ensure a BPR that provides a good balance

between subsonic and supersonic performance, a π_f value of 4.5 was chosen, corresponding to a BPR of 0.7. Therefore, the specific thrust was approximately 835.05 $\frac{Ns}{kg}$ while the specific consumption was 25.2 $\frac{mg}{Ns}$.

Table 8. On-design results.

On-Design Results		
Parameter	**Symbol**	**Value**
Compressor pressure ratio	π_c	30
Fan pressure ratio	π_f	4.5
LP compressor ratio	π_{cL}	5
HP compressor ratio	π_{cH}	6
By-Pass Ratio (BPR)	α	0.7
Turbine Inlet Temperature (TIT)	$T_{t4,\,max}$	2000 K
Air mass flow rate	$\dot{m}_0$	82 kg/s
Core mixer Mach number	M_6	0.5
Fuel heating value	h_{PR}	43.260 MJ/kg
Cooling fractions	$\epsilon_{1,2}$	6.38%
Power extraction	P_{TO}	240 kW
Uninstalled thrust	F	68 kN
Specific fuel consumption	S	25.2 mg/Ns

Since the parametric analysis considers uninstalled thrust, the selected specific thrust value was chosen to provide an approximately 10% margin over the requirement, which, instead, refers to installed thrust [47]. This margin accounts for preliminary considerations of pressure loss and air distortion supplied to the engine, which negatively impact thrust and fuel consumption. Additionally, for initial approximations, the biofuel was assumed to have the same heating value as JP-4. This assumption was based on the "drop-in" requirement, which means that biofuels must ensure the same chemical properties of conventional fuels to be certified. Future updates to the model may include a more precise characterization of the biofuel to better estimate its impact on the propulsion system.

5.2. Off-Design Analysis

Based on the results in Table 8, the off-design analysis was conducted by scaling the component maps using the matrix iteration method and the Newton–Raphson algorithm to solve the nonlinear system of the six power balancing equations of the engine [63]. The off-design data were used to create a propulsive database, which includes the converging solutions for thrust and thrust-specific fuel consumption (TSFC) that varies with flight Mach number, altitude, and throttle settings with respect to the reference condition. Figure 13 shows the performance maps derived from this data set at full throttle.

Figure 13a reports the variation in actual thrust to sea level thrust with respect to the flight Mach number at different altitudes. It is possible to observe that as the Mach number increased, the thrust initially decreased and later increased, likely due to the effect of the ram pressure ratio. Additionally, as expected, the thrust decreased with altitude because of the reduced air density. Figure 13b illustrates the variation in TSFC, which decreased with altitude and significantly increased with flight speed. Figure 14 shows the variation in the thrust-to-maximum thrust ratio with throttle, ranging from 100% to 70%, as the Mach number changed under subsonic flight conditions. The throttle variation was simplified by associating it directly with changes in TIT relative to the maximum allowable turbine temperature. This approach seemed to result in an excessive reduction in thrust with throttle adjustments. Therefore, more precise modeling could be incorporated into future algorithm improvements.

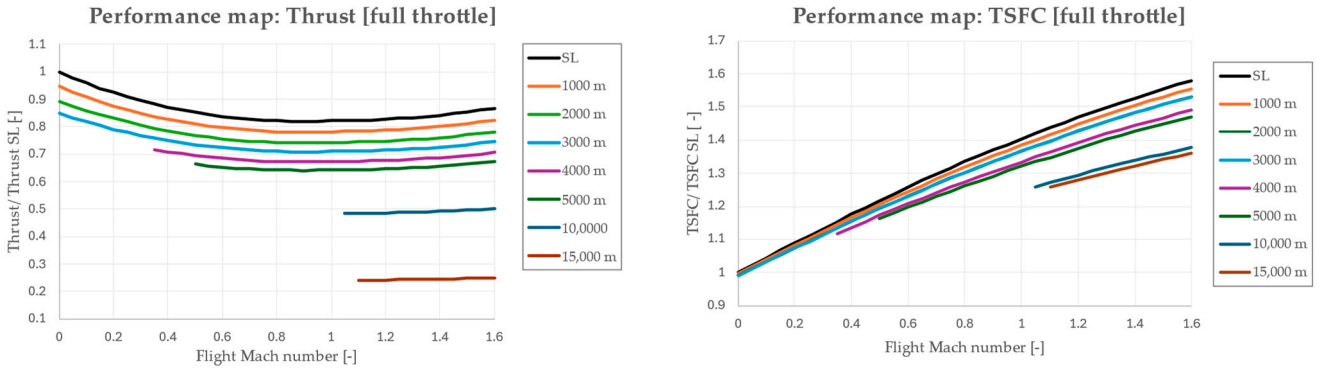

(**a**) (**b**)

Figure 13. Performance maps at full throttle of mixed-flow turbofan engine model for Mach 1.5 case-study: (**a**) thrust versus flight Mach number at different altitudes; (**b**) TSFC versus flight Mach number at different altitudes.

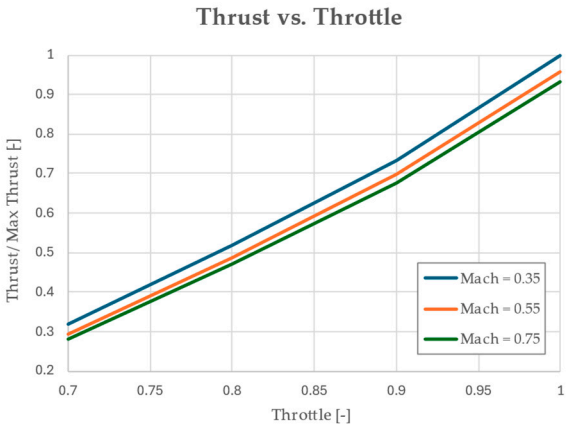

Figure 14. Thrust versus throttle at different flight Mach number under subsonic flight conditions.

5.3. Validation

The proposed engine modelhas beendeveloped in Matlab 9.14 and has been validated by comparing the on-design and off-design analyses results for a mixed-flow turbofan engine with the open-source software GSP 11 [28], which offers several pre-set models ready for simulation. Therefore, the developed model was tuned to simulate the proposed GSP 11 turbofan with mixed exhausts (Figure 15), and the results were then compared to estimate the accuracy of the model.

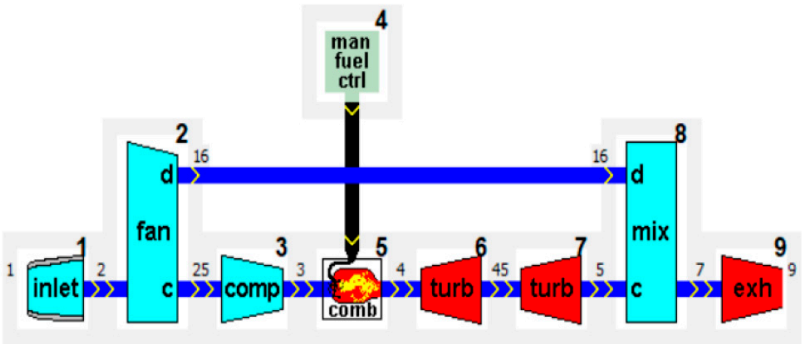

Figure 15. GSP11 mixed-flow turbofan engine model.

The on-design results, presented in Table 9, had a maximum relative error of around 1%, aligning well with the model assumptions and code settings. This error is likely due

to differences in the gas models: the "FAIR" routine uses a generic fuel ($C_{12}H_{23}$) whereas GSP 11 uses a precise model for the specific fuel (Jet-A1 in this case).

Table 9. Comparison of on-design results from the developed model and GSP11.

Parameter	GSP 11	Engine Model	Absolute Error	Relative Error
Thrust [kN]	11.48	11.54	0.06	0.52%
TSFC $\left[\frac{\text{kg}}{\text{Nh}}\right]$	0.0538	0.0541	0.0003	0.51%
Fuel flow $\left[\frac{\text{kg}}{\text{s}}\right]$	0.0172	0.0174	0.002	1.01%
Mixer exit area $[\text{m}^2]$	0.200	0.198	0.002	1.00%

The off-design validation was performed by replicating the engine parameters and settings of the GSP 11 engine model, including component maps. The simulation considered the same reference altitude and flight Mach number as the on-design condition, varying the turbine inlet temperature from 1123 K to 1290 K. The minimum inlet temperature was chosen to avoid surge conditions, which cause simulation divergence, and the same minimum throttle was set in GSP 11. The results are showed in Figure 16.

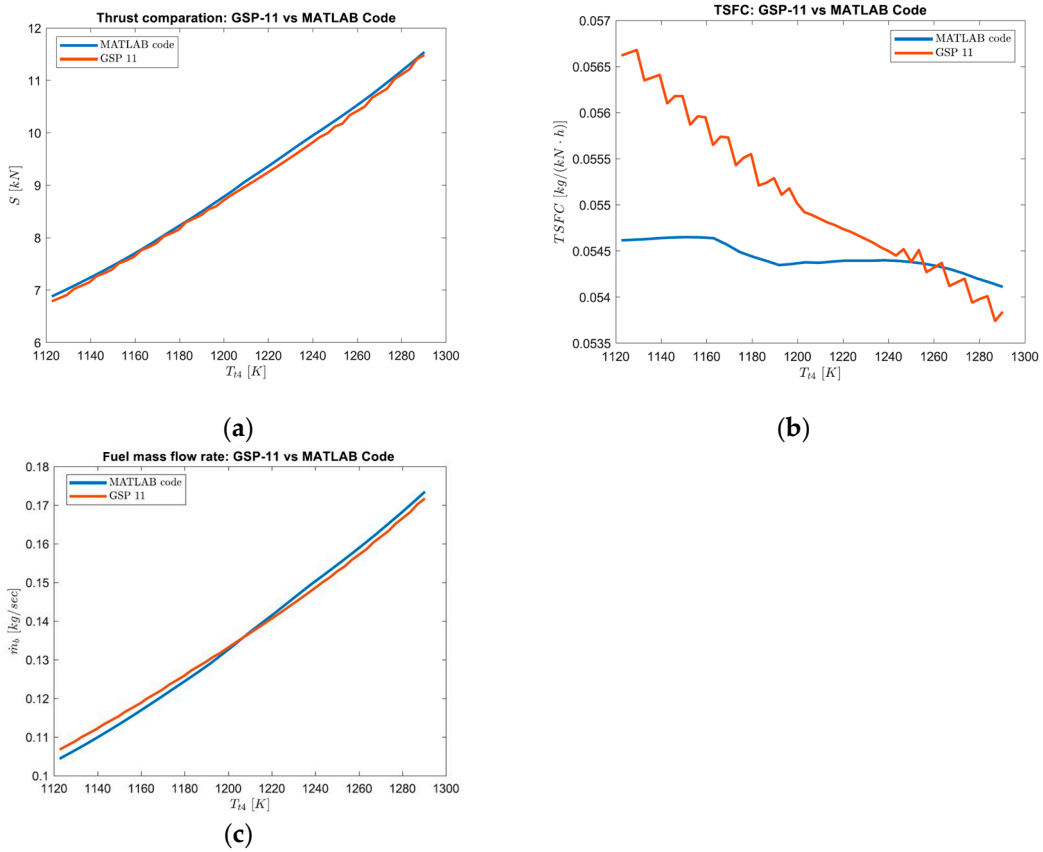

Figure 16. Comparison of off-design results from GSP 11 and engine model developed in Matlab: (**a**) thrust; (**b**) TSFC; (**c**) fuel mass flow rate.

Figure 16a presents the difference between the uninstalled thrust computed using GSP11 and the one predicted using the developed engine model. The comparison indicated that the engine model thrust prediction closely agreed with that of GSP 11 across all temperature settings. However, looking at Figure 16b, the TSFC error appeared to increase for lower temperature settings, reaching a maximum relative error of about 3.5%. The reason behind this behavior was examined considering the definition of TSFC as

$$TSFC = \frac{\dot{m}_b}{T} \tag{41}$$

Therefore, the fuel mass flow rate is also shown in Figure 16c. As illustrated, the two curves closely matched once again. However, a comparison of Figure 16a,c revealed that the Matlab code slightly overestimated the thrust at lower turbine inlet temperatures and underestimated it at higher settings, with the fuel mass flow rate following an inverse trend. These discrepancies led to errors in the TSFC, which was underestimated at lower turbine inlet temperatures and overestimated at higher ones by the Matlab code.

Through this validation, it can be concluded that the code generally demonstrated acceptable accuracy for conceptual design analyses, particularly for on-design conditions. However, under off-design conditions, even small errors in thrust and fuel flow estimates significantly affected TSFC, indicating that its accuracy could be improved. Additionally, further analyses could be conducted by varying other engine control parameters, such as the Mach number and altitude, which were not included in this analysis, to better assess the accuracy of the code under off-design conditions.

6. Mission Simulation

The mission simulation was conducted using the propulsion database generated from the proposed engine model, along with the aerodynamic database developed for the same concept in [64]. Specifically, the trajectory and corresponding performance data were calculated using ASTOS (Analysis, Simulation and Trajectory Optimization Software for Space Applications) by Astos Solutions GmbH (Stuttgart, Germany) [65]. The main results are gathered in Figure 17.

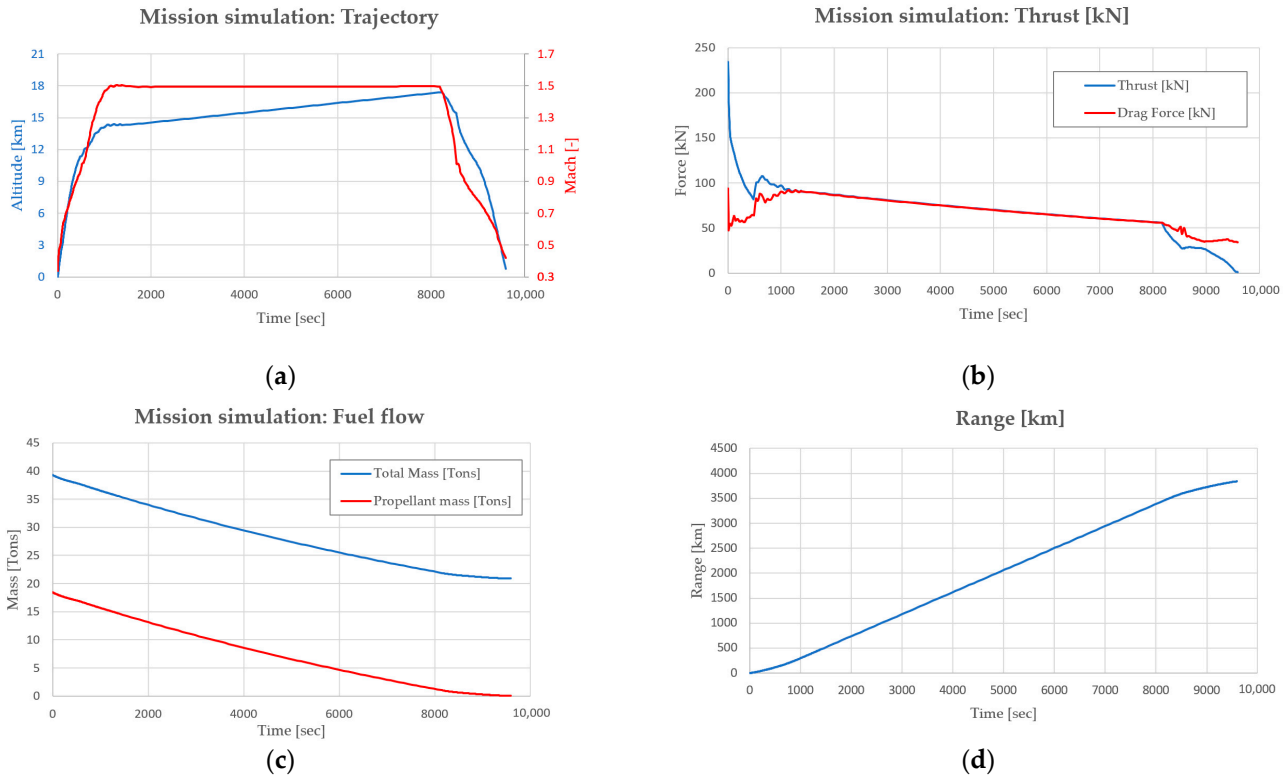

Figure 17. Mission simulation results: (**a**) altitude and Mach number vs. mission time; (**b**) required thrust and available thrust vs. mission time; (**c**) total aircraft mass and propellant mass vs. mission time; (**d**) range vs. mission time.

Figure 17a presents the trajectory, with the mission lasting approximately 4.5 h, divided into 486 points, each representing a step of roughly 32 s. At each time step, a flight Mach

number, altitude, and required thrust are provided. The engine thrust was selected from the propulsive database by adjusting the throttle to achieve the required thrust with a residual of less than 10 N.

Hence, verification of the propulsion system requirement is showed in Figure 17b, where the available thrust (accounting for all engines) was compared with the required thrust, which was estimated considering the drag force of the aircraft. Examining Figure 17b, it is evident that there was excessive thrust during take-off and insufficient thrust during landing. These inaccuracies were likely due to the failure of the model in converging under these off-design conditions. As a result, the software was unable to accurately capture the available thrust conditions to meet the specific requirements. Ultimately, Figure 17c reports the trend in fuel mass and total aircraft mass throughout the mission, while Figure 17d presents the verification of the range requirement (Table 5), which was confirmed to be met.

Emission Estimation

As mentioned above, the main obstacle for the application of the approach suggested in the methodology section, and of correlation methods in general, is the unavailability of LTO emissions data for newly developed and not-yet-certified engines. In this case, the database does not contain supersonic engines and therefore, the reference technology is subsonic and in-flight values were corrected using the variation of the Fuel Flow method available in [30]. Specifically, from the ICAO Aircraft Engine Emissions Databank, the JT8D engine was selected, with its LTO characteristics reported in Figures 18 and 19.

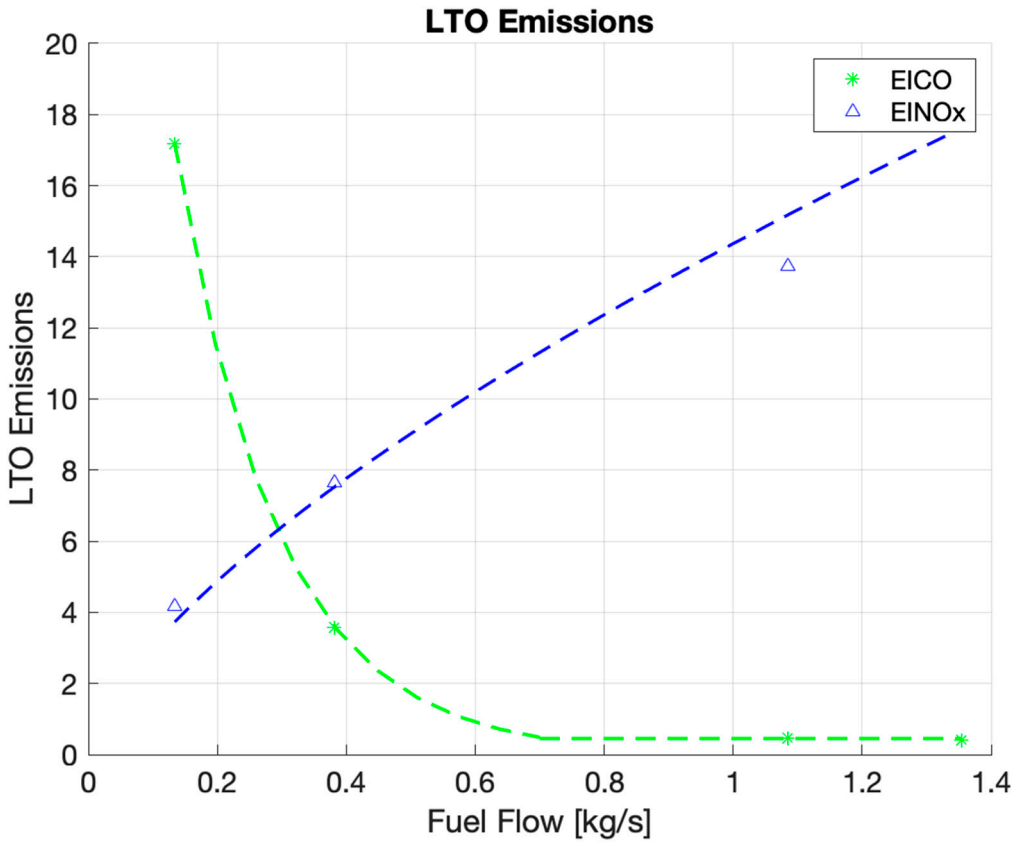

Figure 18. LTO emissions [g/kg] as function of the engine fuel flow for the reference engine.

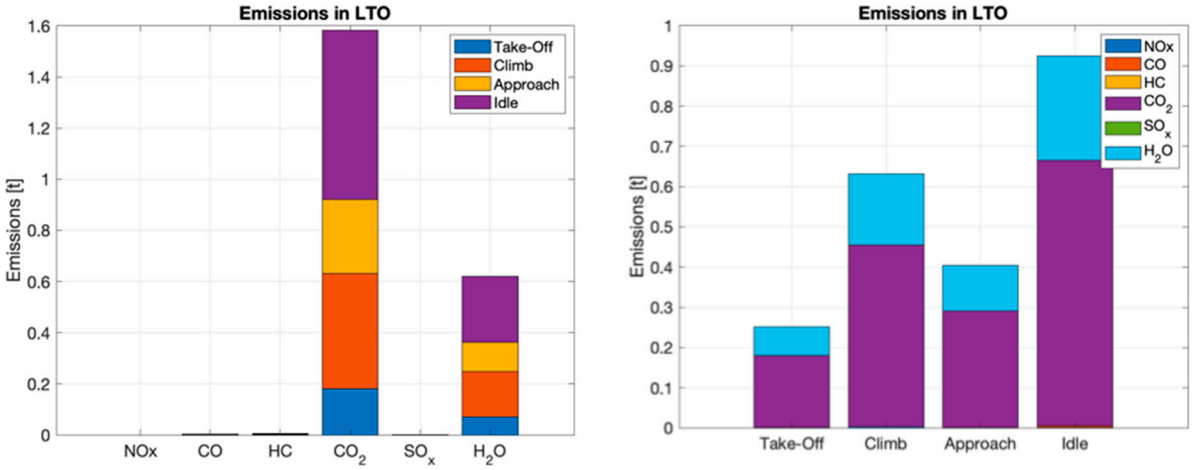

Figure 19. LTO emissions [t]: chemical species and LTO phase breakdown.

Consequently, the application of the Supersonic Fuel Flow method using the fuel flow data from the propulsive database and the trajectory data coming from the preliminary mission simulation, it was possible to obtain the emission index distribution for the non-proportional species, as reported in Figure 20. In this figure, for each point of the reference mission, the emission indexes of CO and NOx were estimated and plotted. Due to the peculiarities of the reference engine used to retrieve the LTO cycle data, no HCs were produced even when varying the throttle setting. As far as the CO index was concerned, the peak values were obtained during the approach and landing phases, as expected, i.e., when the aircraft was operating far away from its optimal design point. Conversely the CO index remained at very low levels and was almost constant for the entire mission. A different behavior was reported for NOx, whose peak value was achieved during the take-off operations, when the engine was operating at its maximum thrust, and therefore when the temperature in the combustion chamber was highest. Then, NOx emissions tended to decrease throughout the mission duration.

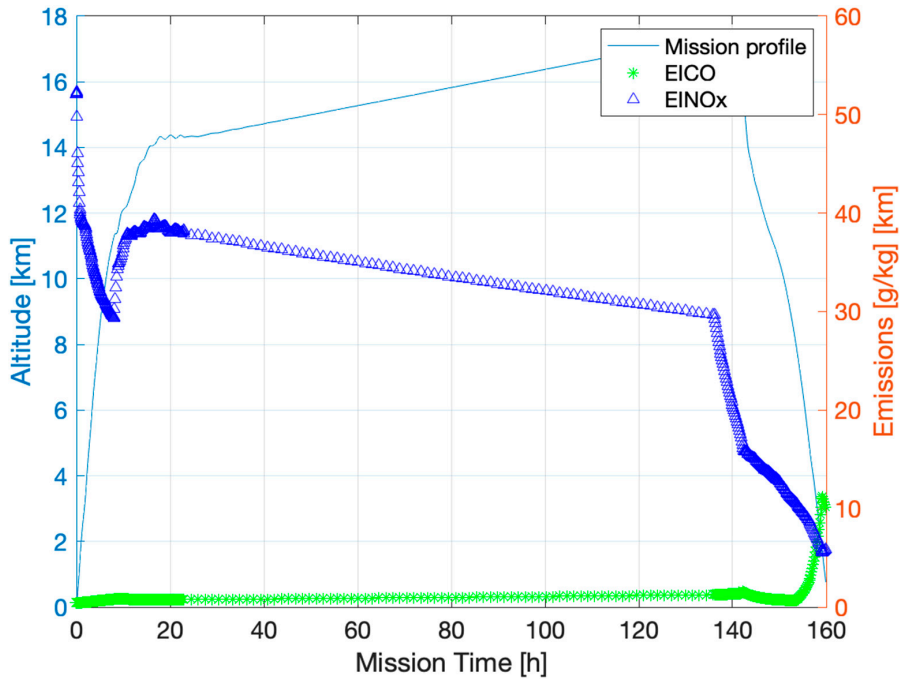

Figure 20. Emission index distribution throughout the reference mission.

7. Conclusions and Future Work

This study highlights the importance of designing an appropriate propulsion system for future sustainable supersonic aircraft, as it significantly impacts both their environmental sustainability and economic viability.

To address the technical implications of environmental requirements for propulsion systems and the vehicle overall from the outset of the design process, integrating a flexible and adaptable engine model tailored specifically for commercial supersonic transport is fundamental. Therefore, a model for mixed-flow, cooled, two-spool, turbofan engines coupled with emission estimations routines was proposed. Unlike other models cited in the literature, the model proposed in this paper was designed for rapid application in the conceptual design of future supersonic aircraft. It allows for fast engine design based on aircraft high-level requirements and integrates emission estimation from the start of the design process. This integration contrasts with other approaches found in the literature, where emission estimation is typically handled by separate tools without direct connection to the engine design.

A parametric analysis varying the cruise Mach number from 1.5 to 3 was performed to analyze the limitations of the algorithm and engine cycle. The results were then compared to the results from the literature. A restriction in the range of overall pressure ratio π_c and fan pressure ratio π_f (and the related BPR) was observed as the Mach number increased. This suggests that the model applicability at Mach 3 may be limited, necessitating further study and potentially the consideration of a VCE model for this flight regime. The complete methodology was then applied to a low-boom Mach 1.5 case study. The engine model was used for both the on-design and off-design analyses, with its accuracy validated against GSP 11 results for a generic mixed-flow turbofan engine, achieving a relative error of about 0.5% in estimating the thrust and TSFC. Subsequently, a propulsion database was generated, gathering the converging solutions of the off-design simulations to enable mission simulation and emission estimation. Specifically, an initial emission estimation was provided in terms of emission indices by applying a modified version of the BFFM2 for sustainable supersonic aircraft. The conceptual design process proved successful, as the aircraft met the initially defined high-level requirements.

However, there remains room for future improvements. Additional analyses should be conducted to carefully verify the behavior of the engine model during take-off and landing conditions. Furthermore, future enhancements of the gas model could be achieved by updating the model and adapting the coefficients of the 7th degree polynomial for non-hydrocarbon fuels. This adaptability would expand the applicability of the engine model to a broader range of fuels, making it even more interesting for studying sustainable supersonic aircraft concepts.

Author Contributions: Conceptualization, G.P., D.F., R.F. and N.V.; methodology, G.P. and R.F.; software, G.P., A.G. and R.F.; validation, G.P.; formal analysis, G.P., A.G. and R.F.; investigation, G.P., A.G. and R.F.; resources, D.F. and N.V.; data curation, G.P., A.G. and R.F.; writing—original draft preparation, G.P., A.G. and R.F.; writing—review and editing, R.F. and D.F.; visualization, G.P., A.G. and R.F.; supervision, R.F. and D.F.; project administration, N.V.; funding acquisition, N.V. All authors have read and agreed to the published version of the manuscript.

Funding: This work has been carried out within the frame of "MDO and REgulations for Low boom and Environmentally Sustainable Supersonic aviation" (MORE&LESS) project. This project has received funding from the European Union's Horizon 2020 research and innovation program under grant agreement No. 101006856.

Data Availability Statement: All data used for this paper are either available within the cited references or embedded in the manuscript.

Acknowledgments: The authors would like to thank Francesco Piccionello for his valuable support provided during his MSc thesis period.

Conflicts of Interest: The authors declare no conflicts of interest.

Abbreviations

ASTRID	Aircraft on-board Systems sizing and TRade-off analysis in Initial Design
BFFM2	Boeing Fuel Flow Method 2
BPR	By-Pass Ratio
EICO	Emission Index of Carbon Monoxide
EIHC	Emission Index of Hydrocarbons
EINOx	Emission Index of Nitrogen Oxides
ESATTO	Environmentally Sustainable AircrafT Trajectory and Operations
GSP	Gas turbine Simulation Program
ICAO	International Civil Aviation Organization
IFV	Inverting Flow Valve
MORE&LESS	MDO and REgulations for Low-boom and Environmentally Sustainable Supersonic aviation
LTO	Landing and Take-Off
MTOW	Maximum Take-Off Weight
NASA	National Aeronautics and Space Administration
NLR	Netherlands Laboratory Research
NPSS	Numerical Propulsion System Simulation
OEW	Operative Empty Weight
OPR	Overall Pressure Ratio
TBE	Turbine Bypass Engine
TIT	Turbine Inlet Temperature
VCE	Variable Cycle Engine
VSH	Variable Specific Heat
Symbols	
A	Area
C_p	Specific heat at constant pressure
e	Polytropic efficiency
F	Uninstalled thrust
f	Fuel-to-air ratio
h	Static enthalpy
h_{PR}	Fuel heating value
M	Mach number
MFP	Mass Flow rate Parameter
$\dot{m}$	Mass flow rate
P	Pressure
P_{TO}	Power at take-off
P_r	Reduced pressure
R	Gas constant
S	Uninstalled thrust specific fuel consumption
T	Temperature or installed thrust
T_t	Total (or stagnation) temperature
$TSFC$	Installed Thrust Specific Fuel Consumption
T/W	Thrust-to-weight ratio
V	Velocity
W/S_w	Wing loading
α	Bypass ratio
α'	Mixer bypass ratio
β	Bleed air fraction
γ	Ratio of specific heats
ϵ_1	Cooling air #1 mass flow rate
ϵ_2	Cooling air #2 mass flow rate
η	Efficiency
π	Total pressure ratio
τ	Total temperature ratio
ϕ	Entropy function

Subscripts	
air	Air
b	Burner
c	Compressor
cH	High-pressure compressor
cL	Low-pressure compressor
f	Fan
M	Mixer
max	Maximum
mH	Mechanical, high-pressure spool
mL	Mechanical, low-pressure spool
n	Nozzle
prod	Products
SL	Sea level
tH	High-pressure turbine
tL	Low-pressure turbine

References

1. Laurence, K.L.J. Toward a Second-Generation Supersonic Transport. *J. Aircr.* **1974**, *11*, 3–9.
2. Candel, S. Concorde and the Future of Supersonic Transport. *J. Propuls. Power* **2004**, *20*, 59–68. [CrossRef]
3. Commercial Supersonic Technology Project. Available online: https://www.nasa.gov/directorates/armd/aavp/cst/ (accessed on 2 August 2024).
4. Honda, M.; Yoshida, K. D-SEND Project for Low Sonic Boom Design Technology. In Proceedings of the 28th Congress of the International Council of Aeronautical Sciences, Brisbane, Australia, 23–28 September 2012.
5. Yoshida, K. Supersonic drag reduction technology in the scaled supersonic experimental airplane project by JAXA. *Prog. Aerosp. Sci.* **2009**, *45*, 124–146. [CrossRef]
6. MDO and REgulations for Low-Boom and Environmentally Sustainable Supersonic Aviation. 2024. Available online: https://cordis.europa.eu/project/id/101006856/results (accessed on 2 August 2024).
7. SENECA—(LTO) noiSe and EmissioNs of supErsoniC Aircraft. Available online: https://seneca-project.eu/ (accessed on 2 August 2024).
8. Hardeman, A.B.; Maurice, L.Q. Sustainability: Key to enable next generation supersonic passenger flight. *IOP Conf. Ser. Mater. Sci. Eng.* **2020**, *1024*, 012053. [CrossRef]
9. Welge, R.H.; Nelson, C.; Bonet, J. Supersonic Vehicle Systems for the 2020 to 2035 Timeframe. In Proceedings of the 28th AIAA Applied Aerodynamics Conference, Chicago, IL, USA, 28 June–1 July 2010.
10. Villena Munoz, C.; Giordana, B.; Lawson, C.; Riaz, A. Conceptual Design of a Next Generation Supersonic Airliner for Low Noise and Emissions. In Proceedings of the AIAA SciTech Forum 2023, National Harbor, MD, USA, 23–27 January 2023.
11. Berton, J.; Huff, D.; Geiselhart, A.; Seidel, J. Supersonic Technology Concept Aeroplanes for Environmental Studies. In Proceedings of the AIAA SciTech Forum 2020, Orlando, FL, USA, 6–10 January 2020.
12. Mercure, R.A. *Propulsion System Considerations for Future Supersonic Transports: A Global Perspective*; ASME: New York, NY, USA, 1996; p. 18.
13. Strack, W.C.; Morris, S.J. The challenges and opportunities of supersonic transport propulsion technology. In Proceedings of the 24th Joint Propulsion Conference cosponsored by the AIAA, ASME, SAE, and ASEE, Boston, MA, USA, 11–13 July 1988.
14. Szeliga, R.; Allan, R.D. *Advanced Supersonic Technology Propulsion System Study—Final Report*; NASA Lewis Research Centre: Cleveland, OH, USA, 1974.
15. Brear, M.J.; Kerrebrock, J.L.; Epstein, A.H. Propulsion System Requirements for Long Range, Supersonic Aircraft. *ASME J. Fluids Eng.* **2005**, *128*, 370–377. [CrossRef]
16. Rettie, I.H.; Lewis, W.G.E. Design and Development of an Air Intake for a Supersonic Transport Aircraft. *J. Aircr.* **1968**, *5*, 513–521. [CrossRef]
17. Sitt, L.E. *Exhaust Nozzles for Propulsion Systems with Emphasis on Supersonic Cruise Aircraft*; NASA Lewis Research Centre: Cleveland, OH, USA, 1990.
18. Zainul, H.; Praseyto, E. Materials selection in design of structures and engines of supersonic aircrafts: A review. *Mater. Des.* **2013**, *46*, 552–560.
19. Papamoschou, D.; Debiasi, M. Conceptual Development of Quiet Turbofan Engines. *J. Propuls. Power* **2003**, *19*, 161–169. [CrossRef]
20. Speth, R.L.; Eastham, S.D.; Fritz, T.M.; Sanz-Morére, I.; Agarwal, A.; Prashanth, P.; Allroggen, F.; Barrett, S.R.H. *Global Environmental Impact of Supersonic Cruise Aircraft in the Stratosphere*; NASA Glenn Research Centre: Cleveland, OH, USA, 2021.
21. Phillips, B.D.; Health, C.M.; Schmidt, J. System-Level Impact of Propulsive Uncertainties for Low-Boom. In Proceedings of the AIAA AVIATION Forum 2020, Virtual event, 15–19 June 2020.

22. Schuermann, M.; Gaffuri, M.; Horst, P. Multidisciplinary pre-design of supersonic aircraft. *CEAS Aeronaut. J.* **2014**, *6*, 207–216. [CrossRef]
23. Villena Munoz, C.; Lawson, C.; Riaz, A.; Jaron, R. Conceptual Design of Supersonic Aircraft to Investigate Environmental Impact. In Proceedings of the AIAA Scitech 2024 Forum, Orlando, FL, USA, 8–12 January 2024.
24. Lytle, J.K. *The Numerical Propulsion System Simulation: An Overview*; NASA Glenn Research Centre: Cleveland, OH, USA, 2000.
25. Nordqvist, M.; Kareliusson, J.; da Silva, E.R.; Kyprianidis, K.G. Conceptual Design of a Turbofan Engine for a Supersonic Business Jet. In Proceedings of the International Society of Air-Breathing Engines (ISABE), Manchester, UK, 3–8 September 2017.
26. PROOSIS—Propulsion Object-Oriented Simulation Software. Available online: https://www.ecosimpro.com/products/proosis/ (accessed on 2 August 2024).
27. Gas Turb. Available online: https://www.gasturb.com/ (accessed on 2 August 2024).
28. Softly—Gas Turbine Simulation Program (GSP 12). Available online: https://usoftly.ir/product/gas-turbine-simulation-program/ (accessed on 2 August 2024).
29. DuBois, D.; Paynter, G.C. Fuel Flow Method2 for Estimating Aircraft Emissions. *SAE 2006 Trans. J. Aerosp.* **2006**, *115*, 1–14.
30. Fusaro, R.; Viola, N.; Galassini, D. Sustainable Supersonic Fuel Flow Method: An Evolution of the Boeing Fuel Flow Method for Supersonic Aircraft Using Sustainable Aviation Fuels. *Aerospace* **2021**, *8*, 331. [CrossRef]
31. Sun, Y.; Smith, H. Review and prospect of supersonic business jet design. *Prog. Aerosp. Sci.* **2017**, *90*, 12–38. [CrossRef]
32. Henne, P.A. Case for Small Supersonic Civil Aircraft. *J. Aircr.* **2005**, *42*, 765–774. [CrossRef]
33. Dovi, A.R.; Wrenn, G.A.; Barthelemy, J.F.M.; Coen, P.G.; Hall, L.E. Multidisciplinary design integration methodology for a supersonic transport aircraft. *J. Aircr.* **1995**, *32*, 290–296. [CrossRef]
34. Li, W.; Shields, E.; Geiselhart, K. A Mixed-Fidelity Approach for Design of Low-Boom Supersonic Aircraft. *J. Aircarft* **2011**, *48*, 1131–1135. [CrossRef]
35. Roncioni, P.; Marini, M.; Gori, O.; Fusaro, R.; Viola, N. Aerodatabase Development and Integration and Mission Analysis of a Mach 2 Supersonic Civil Aircraft. *Aerospace* **2024**, *11*, 111. [CrossRef]
36. Chandrasekaran, N.; Guha, A. Study of Prediction Methods for NOx Emission from Turbofan Engines. *J. Propuls. Power* **2012**, *28*, 170–180. [CrossRef]
37. Viola, N.; Fusaro, R.; Saccone, G.; Borio, V. Analytical Formulations for Nitrogen Oxides Emissions Estimation of an Air Turbo-Rocket Engine Using Hydrogen. *Aerospace* **2023**, *10*, 909. [CrossRef]
38. Fusaro, R.; Saccone, G.; Viola, N. NOx emissions estimation methodology for air-breathing reusable access to space vehicle in conceptual design. *Acta Astronaut.* **2024**, *216*, 304–317. [CrossRef]
39. Ferretto, D.; Fusaro, R.; Viola, N. A conceptual design tool to support high-speed vehicle design. In Proceedings of the AIAA Aviation 2020 Forum, Virtual event, 15–19 June 2020.
40. Raymer, D.P. *Aircraft Design: A Concpetual Approach*; AIAA Education Series; AIAA: Reston, VA, USA, 2018.
41. Arif, I.; Masud, J.; Javed, A.; Toor, Z.G.; Hassan Raza Shah, S. Analytical Modelling and Validation of a Turbofan Engine at Design Conditions. In Proceedings of the AIAA Scitech 2019 Forum, San Diego, CA, USA, 7–11 January 2019.
42. Schlette, T.; Staudacher, S. Preliminary Design and Analysis of Supersonic Business Jet Engines. *Aerospace* **2022**, *9*, 493. [CrossRef]
43. Becker, R.; Reitenbach, S.; Klein, C.; Otten, T.; Nauroz, M.; Siggel, M. An Integrated Method for Propulsion System Conceptual Design. In Proceedings of the ASME Turbo Expo 2015: Turbine Technical Conference and Exposition, Montreal, QC, Canada, 15–19 June 2015.
44. Häßy, J.; Schmeink, J. Knowledge-based Concpetual Design Methods for Geometry and Mass Estimation of Rubber Aero-engines. In Proceedings of the International Council of the Aeronautical Sciences (ICAS), Stockholm, Sweden, 4–9 September 2022.
45. Hutchinson, R.; Lawrence, J.; Joiner, K.F. Conceptual design and integration of a propulsion system for a supersonic transport aircraft. *Proc. Inst. Mech. Eng. Part G J. Aerosp. Eng.* **2022**, *236*, 583–592. [CrossRef]
46. Berton, J.J.; Haller, W.J.; Senick, P.F.; Scott, J.M.; Seidel, J.A. *A Comparative Propulsion System Analysis for the High-Speed Civil Transport*; NASA/TM—2005-213414; Glenn Research Center: Cleveland, OH, USA, 1995.
47. Mattingly, J.D. *Aircraft Engine Design*; AIAA Educational Series; AIAA: Reston, VA, USA, USA, 2002.
48. Mattingly, J.D.; Heiser, W. Performance Estimation of the Mixed Flow, Afterburning, Cooled, Two-Spool Turbofan Engine with Bleed and Power Extraction. In Proceedings of the AIAA/ASME/SAE/ASEE 22nd Joint Propulsionn Conference, Hunsville, Australia, 16–18 June 1986.
49. Qian, R.; Benwei, L.; Hanqiang, S.; Qing, D.; Wang, Y. Aerodynamic Thermodynamic Modeling and Simulation of Turbofan Engine. *IOP Conf. Ser. Mater. Sci. Eng.* **2019**, *685*, 012024. [CrossRef]
50. Fawke, A.J.; Saravanamuttoo, H.I.H. Digital computer simulation of the dynamic response of a twin-spool turbofan with mixed exhausts. *Aeronaut. J.* **1968**, *77*, 471–478. [CrossRef]
51. Stiuso, G. Tecnica di Simulazione Numerica delle Prestazioni Stazionarie e Transitorie di Turbomotori. Master's, Politecnico di Torino, Torino, Italy, 2019.
52. Nada, T. Performance characterization of different configurations of gas turbine engines. *Propuls. Power Res.* **2014**, *3*, 121–132. [CrossRef]
53. Gordon, S.; McBride, B.J. *Computer Program for Calculation of Complex Chemical Equilibrium Compositions and Applications*; NASA Reference Publication 1311; NASA Lewis Research Center: Cleveland, OH, USA, 1994.
54. NASA. CEARUN. Available online: https://cearun.grc.nasa.gov/ (accessed on 2 August 2024).

55. Mattingly, J.D. *Elements of Gas Turbine*; Tata McGraw-Hill: New York, NY, USA, 2007.
56. Zhao, W.; Huang, C.; Zhao, Q.; Ma, Y.; Xu, J. Performance analysis of a pre-cooled and fuel-rich pre-burned mixed-flow turbofan cycle for high speed vehicles. *Energy* **2018**, *154*, 96–109. [CrossRef]
57. Koff, B.L.; Koff, S.G. Engine design and challenges for the high Mach transport. In Proceedings of the 43rd AIAA/ASME/SAE/ASEE Joint Propulsion Conference & Exhibit, Cincinnati, OH, USA, 8–11 July 2007.
58. Dinc, A. NOx emissions of turbofan powered unmanned aerial vehicle for complete flight cycle. *Chin. J. Aeronaut.* **2020**, *33*, 1683–1691. [CrossRef]
59. Wang, Y.; Yin, H.; Zhang, S.; Yu, X. Multi-objective optimization of aircraft design for emission and cost reductions. *Chin. J. Aeronaut.* **2014**, *27*, 52–58. [CrossRef]
60. ICAO Aircraft Engine Emissions Databank. Available online: https://www.easa.europa.eu/en/domains/environment/icao-aircraft-engine-emissions-databank#:~:text=The%20ICAO%20Aircraft%20Engine%20Emissions,according%20to%20their%20national%20regulations (accessed on 7 August 2024).
61. NASA. Quiet Supersonic Technology (QueSST) Mission. Available online: https://www.nasa.gov/mission/quesst/ (accessed on 2 August 2024).
62. Kishi, Y.; Yashiro, R.; Kanazaki, M. Low-Boom Design for Supersonic Transport with Canard and Forward-Swept Wings Using Equivalent Area Design Method. *Aerospace* **2023**, *10*, 717. [CrossRef]
63. Piccionello, F. Modeling of Propulsion Systems for Supersonic Civil Aircraft. Master's Thesis, Politecnico di Torino, Torino, Italy, 2023.
64. Richiardi, G.; Graziani, S.; Gori, O.; Viola, N. Low-boom supersonic business jet: Aerodynamic analysis and mission simulation towards a CO2 emission standard. In Proceedings of the Aeronautics and Astronautics—AIDAA XXVII International Congress in Materials Research Proceedings, Padova, Italy, 4–7 September 2023.
65. ASTOS Solutions. Available online: https://www.astos.de/products/astos (accessed on 2 August 2024).